Analysis of construction experience of using lightweight cellular concrete as a subbase material

by

Sergey Averyanov

A thesis

presented to the University Of Waterloo

in fulfilment of the

thesis requirement for the degree of

Master of Applied Science

in

Civil Engineering

Waterloo, Ontario, Canada

AUTHOR'S DECLARATION

I hereby declare that I am the sole author of this thesis. This is a true copy of the thesis, including any required final revisions, as accepted by my examiners.

I understand that my thesis may be made electronically available to the public.

ABSTRACT

Canada has the second largest territory in the world and its pavement network has over 1,000,000 km of roads spread over regions with various existing soil types. One of the challenges for engineers is to determine the soil type for a particular road project and to develop a pavement design accordingly. It is very important to identify weak or frost-susceptible soils, as they are influenced greatly by weather conditions which may lead to settlement issues and may affect the overall pavement performance. One viable option to overcome the consequences of settlement problems is the usage of lightweight materials, such as Lightweight Cellular Concrete (LCC), which reduces the effective stress on the underlying soil. This material has a number of advantages including: it is lightweight; exhibits superior thermal properties; is freeze-thaw resistant; has good flowability; is cost-effective; and sustainable.

This study aims to assess LCC in terms of performance in past projects, mechanical properties of LCC from the ongoing project as well as prediction of its field performance in the future. Already existing road sections with the installed LCC as a subbase were studied. The available information from those road sections was compiled and analyzed to establish similarities and differences in the cases as well as challenges and recommendations for LCC installation. All projects were aiming to solve the settlement problem. It is observed that settlement usually occurs on localized parts of the road and not on its whole length. After visual inspection, some of the studied sections, such as Winston Churchill Boulevard and Highway 9 were found to have no severe rutting or fatigue cracking, however, longitudinal and transverse cracking were observed at Dixie Road, particularly at the adjacent section to the Granular base pavement.

The samples from the ongoing site were collected for laboratory testing. Results from the laboratory determined the density of the LCC in the hardened stage as approximately 40 kg/m^3 lower than its plastic density. The similar information was found in the literature. However, compressive strength of the in-situ cast material was determined to be higher than for the similar densities in the previous findings. Modulus of elasticity also differs from the typical values, whereas it was found to be lower. Poisson's ratio values were found to be in the typical range.

To predict the ability of the road sections to bear the designed traffic loads and to predict in-service performance, the case studies with settlement issues were considered. Failure criteria analysis has been conducted. The results of the failure criteria analysis indicated that the usage of LCC as a subbase material is more durable than the conventional granular material with similar thickness. This also shows that using LCC as a subbase layer material could be potentially effective.

ACKNOWLEDGEMENTS

I would first like to thank my supervisor Dr. S.L. Tighe from the Civil and Environmental Engineering Department at the University of Waterloo, for her support and guidance over the course of this research.

I would also like to express my gratitude to my thesis readers Dr. W.C. Xie, from the Department of Civil and Environmental Engineering at The University of Waterloo and Dr. V. Henderson – an adjunct professor from the Department of Civil and Environmental Engineering at the University of Waterloo. Thanks also to the Civil Engineering Department lab technicians, Richard Morrison, Douglas Hirst, Peter Volcic, Ya Ting Yang, and Azka Aqib.

Appreciation is also extended to CEMATRIX and National Sciences and Engineering Research Council (NSERC) for the supply of research materials and funding this project. Special thanks to Dan Hanley, Brad Dolton, Dr. J. Li, Steve Bent, and Cameron Nerland from CEMATRIX for sharing their knowledge during my research.

In addition, I would like to thank my colleagues at the University of Waterloo who contributed their time and effort during my project. Namely, Dr. H. Baaj, Frank Mi-Way Ni, Abimbola Grace Oyeyi, Eskedil Melese, Daniel Pickel, Dahlia Malek, Drew Dutton, Seyedata Nahidi, Frank Liu, Qingfan Liu, Taha Younes, Yashar Azimi Alamdary, Zaid Alyami, Luke Zhao, Taher Baghaee Moghaddam, Jessica Rossi, Beverly Seibel. This work would not have been possible without your help.

DEDICATION

This thesis is dedicated to my family, whose support and love have made this a possibility.

TABLE OF CONTENTS

AUTHOR'S DECLARATION ii
ABSTRACT iii
ACKNOWLEDGEMENTS iv
DEDICATION v
Table of Contents vi
List of Figures ix
List of Tables xi
List of Abbreviations xiii
1 Introduction 1
1.1 Background 2
1.2 Research Hypotheses 3
1.3 Research Scope and Objectives 3
1.4 Thesis Organization 3
2 Literature Review 5
2.1 Lightweight Cellular Concrete (LCC) 5
2.2 Composition of LCC 7
2.3 Properties of LCC 8
2.3.1 Fresh State 8
2.3.2 Hardened State 10
2.4 Challenges 15
2.5 Sustainability 16
2.6 Applications 17
2.7 Applications in Pavement Engineering 18
2.8 Summary of Literature Review and Research Gaps 19
3 Field Performance Review 20
3.1 Methodology 20
3.2 Case Studies 21

3.2.1 Dixie Road. Region of Peel, Caledon, Ontario, Canada 22
3.2.2 Brentwood Light Rail Transit (LRT) Bus-Lane. Calgary, Alberta, Canada 31
3.2.3 Winston Churchill Boulevard. Brampton, Ontario, Canada 34
3.2.4 Highway 9. Holland Marsh, Ontario, Canada 36
3.2.5 View and Vancouver Streets, City of Victoria, British Columbia, Canada 40
3.3 Summary of Case Studies 44
3.4 Discussions and Recommendations 45
4 Pavement Design and Analysis 48
4.1 Introduction into Pavement Design 48
4.2 Pavement Design with Lightweight Cellular Concrete (LCC) 48
4.3 Analysis Method 49
4.4 Failure Criteria Analysis 50
4.4.1 First Approach 51
4.4.2 Second Approach 55
4.4.3 Third Approach 59
4.5 Summary 65
5 Toronto Project 66
5.1 Site Description 66
5.2 Approach 67
5.3 Production and Placement 67
5.4 Laboratory Tests 69
5.4.1 Unconfined Compressive Strength 70
5.4.2 Modulus of Elasticity and Poisson's Ratio 74
5.4.3 Relationship between Properties 76
5.5 Summary 77
6 Conclusions and Future Recommendations 78
6.1 Conclusions 78
6.2 Future Recommendations 79
References 81

Appendix I……86

Appendix II……89

Appendix III……..91

LIST OF FIGURES

Figure 1-1: Typical Cross Section of a Rural Conventional Asphalt Concrete Pavement (TAC, 2013) 1

Figure 2-1: Texture of Wet LCC (Maher and Hagan, 2016) 6

Figure 2-2: "Wet" Mix Equipment (Dolton et al., 2016) 6

Figure 2-3: “Dry” Mix Equipment (Dolton et al., 2016) 7

Figure 2-4: Instability Issues with Ultra-Low Density LCC (Field Performance) 9

Figure 2-5: Lightweight Cellular Concrete being Placed with a Flexible Hose (Taylor et al., 2016) 10

Figure 2-6: Splitting Tensile Strength Test Setup 12

Figure 2-7: Global Use of Cellular Concrete (Oginni, 2015) 17

Figure 3-1: Overview of Research Methodology 21

Figure 3-2: Road Section Location (Google maps, 2018) 22

Figure 3-3: Typical Cellular Cross Section (Griffiths and Popik, 2013) 23

Figure 3-4: Construction Process of Dixie Road, Region of Peel, Caledon, Ontario, Canada (CEMATRIX) 24

Figure 3-5: Condition of Dixie Road, Region of Peel, Caledon, Ontario, Canada 25

Figure 3-6: Ground Penetrating Radar Equipment 26

Figure 3-7: GPR Longitudinal Image of Southbound Lane, L10 (Griffiths and Popik, 2013) 27

Figure 3-8: GPR Transverse Images at Longitudinal Crack Locations, L4, and L5 (Griffiths and Popik, 2013) 28

Figure 3-9: FWD Truck and Trailer (Griffiths and Popik, 2013) 28

Figure 3-10: Structural Number Comparison Plot (Griffiths and Popik, 2013) 29

Figure 3-11: Site Location (Google Maps, 2018) 31

Figure 3-12: Bus Lane. (a) Reconstruction Process. Placing the LCC (CEMATRIX) (b) After Installing the LCC Layer (CEMATRIX) 32

Figure 3-13: Pavement Distresses on the non-LCC section - 1(CEMATRIX, 2018)..... 33

Figure 3-14: Pavement Distresses on the non-LCC section - 2(CEMATRIX, 2018)..... 33

Figure 3-15: Location of the Road Section (Google Maps, 2018)..... 34

Figure 3-16: Pavement Structure. Winston Churchill Boulevard (CEMATRIX)..... 35
Figure 3-17: Condition of Winston Churchill Boulevard, August 2017..... 35
Figure 3-18: Highway 9 Site Location (Google Maps, 2018) 36
Figure 3-19: Highway 9 Site Location with the Local Landscape (Google Maps, 2018) 36
Figure 3-20: Highway 9 Construction Process (CEMATRIX)..... 38
Figure 3-21: Condition of Highway 9, Three Years after Construction 39
Figure 3-22: Condition of Highway 9, Three Years after Construction 39
Figure 3-23: Site location. (Google maps, 2018)..... 40
Figure 3-24: View Street and Vancouver Street Construction Process. Wet Mix Equipment (CEMATRIX) 41
Figure 3-25: Benkelman Beam Deflection Testing 42
Figure 4-1: Pavement Structure with LCC..... 49
Figure 4-2: Vertical and Tensile Stresses. Comparison for Dixie Road, Highway 9 and Winston Churchill Blvd (WESLEA software, 2018) 54
Figure 4-3: Allowable Number of Load Repetition. Fatigue Cracking and Rutting for Dixie Road, Highway 9 and Winston Churchill Blvd (WESLEA software, 2018)..... 58
Figure 4-4: Predicted Damage. Fatigue Cracking and Rutting for Dixie Road, Highway 9 and Winston Churchill Blvd (WESLEA Software, 2018)..... 64
Figure 5-1: Site Location (Google Maps, 2018) 67
Figure 5-2: Construction Process. Toronto, May 2018..... 68
Figure 5-3: Samples, Collected on Site..... 69
Figure 5-4: Weather Forecast during Construction and Casting the Samples 70
Figure 5-5: Unconfined Compressive Strength..... 71
Figure 5-6: UCS Test Results 72
Figure 5-7: Average UCS Test Results..... 73
Figure 5-8: Modulus of Elasticity and Poisson's Ratio Test Setup 75
Figure 5-9: Modulus of Elasticity Test Results for 28 Days Samples 76
Figure 5-10: Correlation of Compressive Strength and Density..... 77

LIST OF TABLES

Table 2-1: Typical Properties of LCC Based on British Concrete Association (BCA, 1994). 11

Table 2-2: Empirical Model for Cellular Concrete Modulus of Elasticity Determination (Amran, Farzadnia and Ali, 2015) 13

Table 2-3: Summary of Cellular Concrete Applications Based on Density (Sari and Sani, 2017) 18

Table 3-1: Comparison of Pavement Structures 27

Table 3-2: Project Specifications and QC Results (Maher and Hagan, 2016)..... 38

Table 3-3: Benkelman Beam Results (Golder Associates Ltd. Report, 2008)..... 42

Table 3-4: FWD Test Data..... 43

Table 3-5: Summary of the Available Cases of Using LCC as a Subbase Material in Pavement Construction in Canada..... 44

Table 4-1: WESLEA Settings for Dixie Road, Highway 9 and Winston Churchill Boulevard (Material Properties of the Pavement) 50

Table 4-2: ESALs for Three Road Sections in Ontario 51

Table 4-3: Vertical and Tensile Stresses. Dixie Road..... 51

Table 4-4: Vertical and Tensile Stresses. Highway 9 52

Table 4-5: Vertical and Tensile Stresses. Winston Churchill Blvd 52

Table 4-6: Allowable Number of Load Repetition. Fatigue Cracking and Rutting for Dixie Road 55

Table 4-7: Allowable Number of Load Repetition. Fatigue Cracking and Rutting for Highway 9..... 56

Table 4-8: Allowable Number of Load Repetition. Fatigue Cracking and Rutting for Winston Churchill Boulevard..... 56

Table 4-9: Predicted Damage (Fatigue Cracking and Rutting) of Pavement with Granular B Subbase. Dixie Road (WESLEA, 2018) 60

Table 4-10: Predicted Damage (Fatigue Cracking and Rutting) of Pavement with LCC Subbase. Dixie Road (WESLEA, 2018)..... 60

Table 4-11: Predicted Damage (Fatigue Cracking and Rutting) of Pavement with Granular Subbase. Highway 9 (WESLEA, 2018)..... 61

Table 4-12: Predicted Damage (Fatigue Cracking and Rutting) of Pavement with LCC Subbase. Highway 9 (WESLEA, 2018) 61

Table 4-13: Predicted Damage (Fatigue Cracking and Rutting) of Pavement with Granular Subbase. Winston Churchill Boulevard (WESLEA, 2018) 62

Table 4-14: Predicted Damage (Fatigue Cracking and Rutting) of Pavement with LCC Subbase. Winston Churchill Boulevard (WESLEA, 2018) 62

Table 5-1: Typical Properties of Cellular Concrete Based on British Concrete Association (BCA 1994) 73

LIST OF ABBREVIATIONS

AADT	Average Annual Daily Traffic
AASHTO	American Association of State Highway and Transportation Officials
ACD	Activity Cycle Diagram
ARA	Applied Research Associates
ASTM	American Standards Tests and Methods
BCA	British Concrete Association
CBR	California Bearing Ratio
CPATT	Centre for Pavement and Transportation Technology
ESAL	Equivalent Axle Single Load
FWD	Falling Weight Deflectometer
GPR	Ground Penetrating Radar
HMA	Hot Mix Asphalt
PC	Portland Cement
LCC	Lightweight Cellular Concrete
LCCA	Life-Cycle Cost Analysis
LVDT	Linear Variable Displacement Transducers
LRT	Light Rail Transit
MEPDG	Mechanistic-Empirical Pavement Design Guide
MTO	Ministry of Transportation Ontario
RAP	Recycled Asphalt Pavement
RCA	Recycled Concrete Aggregate
SCC	Self Consolidating Concrete
TAC	Transportation Association of Canada
QA	Quality Assurance
QC	Quality Control
UCS	Unconfined Compressive Strength

CHAPTER 1

1 INTRODUCTION

Canada has the second largest territory in the world and its pavement network has over 1,000,000 km of roads (TAC, 2013). The typical pavement structure in Canada consists of a surface layer, which can be made up of bituminous layers or rigid concrete layers, a granular base and a subbase overlying the subgrade (Figure 1-1). The main purpose of the layers is to support the wheel loads from traffic and distribute it to the underlying subgrade. When designing pavement, it is very important to take into consideration: thickness of each layer; volume and composition of traffic; climate; range of construction materials available; desired serviceable life; and subgrade type and strength (TAC, 2013).

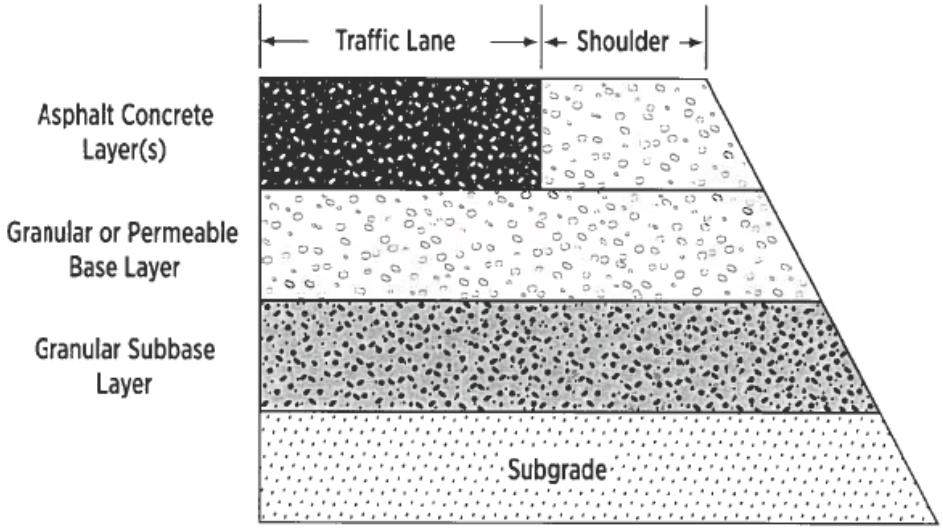

Figure 1-1: Typical Cross Section of a Rural Conventional Asphalt Concrete Pavement (TAC, 2013)

The subgrade type is a very significant factor because Canada's road network is spread over regions with various existing soil types. Some of these soil types, such as weak or frost-susceptible soils are referred to as difficult geotechnical conditions. In addition to the type of soil, serious temperature fluctuations in winter months, as well as thawing during spring months, play a significant role in pavement performance with respect to the subgrade. Frost heave in winter months as well as thawing during spring months influences the settlement of pavements and reduces bearing capacity of the pavement layers. Materials that are commonly used in the subbase layer include unbound granular materials, which have low insulation

properties and may lead to penetration of frost through the pavement structure straight to the subgrade (Hoff et al., 2002).

As a result of having unbound granular materials in a subbase, water can easily penetrate through the pavement structure into the subgrade and saturate the underlying soils. Thus, during the freeze-thaw cycles, those soils may become unstable, leading to settlement and causing distresses to the whole pavement structure (Hoff et al., 2002). To address this problem, it is recommended to remove weak organic soils from exposed subgrade areas prior to placement of embankment materials. In some cases, it is time-consuming and not economically beneficial, to replace these weak soils with stiff and stable materials or pavement structure. Another feasible solution may be using geosynthetics, including geotextiles, geofabrics, and geogrids, to provide "bridge" embankments over thick deposits of these organic-rich soils (TAC, 2013).

In order to overcome settlement issues due to excessive weight of pavement, the following materials may be utilized: (TAC, 2013)

- Expanded polystyrene
- Expanded lightweight clay
- Air cooled blast furnace slag
- Recycled Concrete Aggregates (RCA)
- Reclaimed Asphalt Pavement (RAP)
- Waste glass and ceramic

To address the problem of weak soils, and to mitigate settlement and fast deterioration of the pavements, Lightweight Cellular Concrete (LCC) is considered as another potential solution. For a better understanding of the benefits and drawbacks of using LCC, as well as performance evaluation of the pavement structure, analysis of construction experience of using LCC as a subbase material has been performed in this research.

1.1 Background

LCC, sometimes referred to as "foamed concrete" or "aerated concrete", is a useful construction material with many applications. It differs from conventional concrete in that it does not contain any coarse aggregate. Instead, it is made from a mixture of cement and water that is mixed with a foaming compound to generate a matrix of small air bubbles, which makes the concrete extremely lightweight. Apart from being lightweight, LCC is a cost-effective and sustainable material and has superior thermal properties, freeze-thaw resistance, and good flowability. LCC technology was originally developed in Sweden in the early 1900s, but was not put into commercial use until after World War 2. More recently, technological advances in LCC have led to its use for various applications. Today, LCC is used in areas that require strong, yet lightweight and inexpensive materials. Commonly, LCC is used as a lightweight fill material

in embankments and beneath roads, or as an energy-absorbing material. Though many of its properties are still not thoroughly studied, the usage of LCC is becoming more popular in construction projects in North America and abroad.

For the most part, lightweight fill materials are progressively utilized in civil engineering purposes such as backfilling, slope stabilization, embankment fills, and pipe bedding (Horpibulsuk et al., 2014). The main intent of lightweight fill materials is to be used as an alternative construction material that significantly reduce the weight of fills, thereby mitigating excessive settlements and bearing failures. This can subsequently result in more economic designs for structures such as retaining walls and base layers of roadways.

1.2 Research Hypotheses

The primary hypotheses of this research are as follows:

- Pavement structures with already installed LCC as a subbase can exhibit result in good pavement performance
- Pavement performance of LCC pavement can be predicted using WESLEA analysis
- Mechanical properties of LCC samples cast in-situ are different from the typical values in the literature

1.3 Research Scope and Objectives

The scope of this project is to review the condition and performance of existing road sections that were constructed using LCC as well as to evaluate the mechanical properties of this material during the construction. This methodology will enable the prediction of future performance. To achieve this goal, the specific objectives are as follows:

1. Assess the condition of existing pavement sections with LCC as a subbase material
2. Conduct an analysis of the LCC performance of the existing roads
3. Determine structural properties of in-situ LCC

1.4 Thesis Organization

The components of the thesis include outline of scope and objectives, literature review, review of case studies, performance evaluation of LCC in past and current projects and prediction of the future performance (failure criteria analysis). At the end of the thesis, conclusions and recommendations will be provided.

This thesis is organized into six Chapters.

Chapter 1 explains the scope and objectives of the research project and provides the thesis organization.

Chapter 2 provides an extensive review of the literature related to Lightweight Cellular Concrete, its composition and properties. Fresh and hardened states of LCC are presented by various mechanical properties of the material. This Chapter covers methods of producing LCC and presents benefits and drawbacks of this material. In addition, potential sustainable benefits from using LCC are presented in this Chapter. Number of applications of LCC are presented in Chapter 1, as well as applications in pavement engineering. Research gaps are also described in this Chapter.

Chapter 3 presents case studies of using LCC as a subbase material in pavement engineering across Canada. This Chapter describes each of the cases separately by discussing the location of the site, problem, possible solutions to the issue, construction process, results and tests that were done after construction. At the end of the Chapter, a table summarizing all of the case studies is presented. The most crucial issues that future contractors could potentially face, as well as recommendations, are discussed in Chapter 3.

Chapter 4 describes performance prediction analysis by introducing failure criteria. Three case studies from the previous Chapter were taken as the examples of pavement structure and were analyzed on bearing capacity of the layer, ability of the pavement to resist fatigue cracking and rutting issues, and potential number of ESALs that the pavement could potentially preserve without any maintenance.

Chapter 5 provides the results of the laboratory testing of the samples collected from the ongoing Toronto project. Site and project details are described in this Chapter. The tests were conducted at the Centre for Pavement and Transportation Technology (CPATT). The laboratory results were analyzed and correlation between the properties was made. Values, obtained from the laboratory work were compared to the typical values for LCC in the literature.

Chapter 6 contains the conclusions and recommendations based on the research conducted for the thesis.

CHAPTER 2

2 LITERATURE REVIEW

This Chapter provides a summary of the relevant literature related to this thesis. It describes composition, methods of production, mechanical properties and applications of Lightweight Cellular Concrete (LCC).

2.1 Lightweight Cellular Concrete (LCC)

ASTM C796 (2012) defines LCC as:
"A lightweight product consisting of Portland Cement, cement-silica, cement-pozzolan, lime-pozzolan, or lime-silica pastes, or pastes containing blends of these ingredients and having a homogeneous void or cell structure, attained with gas-forming chemicals or foaming agents (for cellular concretes containing binder ingredients other than, or in addition to Portland Cement, autoclave curing is usually employed)".

Cellular concrete is relatively homogeneous compared to conventional concrete, as it does not contain coarse aggregate, so there is limited variation in its properties. The properties of Lightweight Cellular Concrete (LCC) depend on its microstructure and composition, methods of pore-formation and curing. LCC is lightweight, easy to construct, and economical in terms of transportation. LCC is comprised of cement or lime mortar matrix, in which air-voids are entrapped by a suitable aerating agent (Ramamurthy, Nambiar and Ranjiani, 2009). Traditional concrete mix components densities may vary between 1000 kg/m^3 (water) and 3200 kg/m^3 (cement) (Darshan, 2016). By appropriate method of production, LCC densities are considerably lower, ranging from 250 kg/m^3 to 1800 kg/m^3, but typically between 400 kg/m^3 and 600 kg/m^3 (Dolton et al., 2016). This makes LCC desirable as a very low-density material. The cellular pore network of LCC also provides a high degree of thermal insulation, as well as considerable savings in material. Figure 2-1 shows the texture of wet LCC as it is being placed from a pipe.

Figure 2-1: Texture of Wet LCC (Maher and Hagan, 2016)

LCC can be produced in two different ways: “dry” mix or “wet” mix. Figure 2-2 shows “wet” mix process, where cement, water, and admixtures are pre-batched into a slurry and sent to site in trucks. Once on site, the temperature, density, and viscosity of the slurry is measured to confirm compliance with the requirements to make LCC. After quality is verified, the slurry is delivered into the LCC equipment, which then injects foam into the slurry and pumps the LCC into place (CEMATRIX, 2018). The “dry” mix process is better for high-volume projects (Figure 2-3). All the components are blended on site to form the slurry, then foam is injected and the concrete is pumped into place (Dolton et al., 2016). With a skilled and experienced construction team, installation is usually quick and inexpensive. Those two factors usually come as a significant part of the overall project cost (Loewen, Baril, and Eric, 2012).

Figure 2-2: "Wet" Mix Equipment (Dolton et al., 2016)

Figure 2-3: "Dry" Mix Equipment (Dolton et al., 2016)

2.2 Composition of LCC

LCC is typically composed of Portland Cement, water, pre-formed foaming agent, with no coarse aggregate. Sometimes pozzolan materials such as fly ash, silica fume, slag, or various chemical admixtures are also included (Ozlutas, 2015).

Portland Cement

The main cementitious component of LCC is Portland Cement. The content is approximately 300-400 kg/m^3 in the lightweight cellular concrete mix and it can vary depending on the desired density and strength of the final product (Jones, 2001)**.**

Pozzolan Materials

Pozzolans are a broad class of siliceous or siliceous and aluminous materials, which, in themselves, possess little or no cementitious value. In order to improve compressive and flexural strength, reduce cost, heat of hydration, drying shrinkage, thermal conductivity and sustainability, fly ash, blast furnace slag or silica fume may be added to PC (Dolton et al., 2016; Kearsley and Wainwright 2001; 2002). Jones et al. (2017) stated that replacing Portland Cement with fly ash up to 40% could significantly reduce the embodied carbon dioxide by 65% compared to the 100% Portland Cement mix while has a similar 28-day compressive strength (0.25 MPa compared to 0.31 MPa). However, the drawbacks of using fly ash are the slow rate of strength gain, and it might cause foam instability as the water demand may increase (Ozlutas, 2015).

Fine Aggregates

Fine sand typically is composed of 2mm maximum size aggregates for use in LCC with dry densities equal to or greater than 600kg/m^3. In lower density LCC, fillers like fly ash can be used instead (BCA, 1994; Dransfield, 2000). Carbon nanotubes (CNTs) have also been incorporated to LCC mix as fillers for support. They are found to develop more homogenous cell structure with closed cell bubbles (Yakovlev et al., 2006). However, CNTs can form clumps and ultimately cause foam instability, this will require dispersion in water which might not prove effective (Ozlutas, 2015).

Water

The cement to water ratio used for LCC ranges from 0.4 to 1.25 (Kearsley, 1996). It must be noted that the quantity of water required is dependent on the composition and use of the material which relies on consistency and stability (Ramamurthy, Nambiar and Ranjani, 2009). Excess water in the mix leads to segregation while insufficient water content may collapse the mix (Nambiar and Ramamurthy, 2006).

Foam

A foaming agent is usually added to the base mix (cement slurry) to produce the bubble structure in the LCC material. Foaming agents can either be blended with the base mix after they have been produced separately or mixed along with the ingredients for the base mix (Byun, Song and Park, 1998). The former is being used more often. The main requirement is that the foaming agent be stable and firm in order to resist mortar pressure (Koudriashoff, 1949). Foam can either be wet or dry. Studies have reported stability issues with the wet foam producing bubble sizes of between 2 mm to 5 mm. However, dry foam is reported to have more reliability in terms of stability with bubble sizes of 1mm (Aldridge, 2005). Examples of foaming agents include detergents, resin soap, hydrolized protein, saponin, and neopar (Ramamurthy, Nambiar and Ranjani, 2009; Valore, 1954a).

2.3 Properties of LCC

2.3.1 Fresh State

Fresh state of cellular concrete is described as free-flowing, self-leveling and self-compacting. The higher the air volume in the LCC is, the easier it is to place it. In addition, it does not need further consolidation during placement (Ozlutas, 2015). However, in some mixes with the increased volume of the air, cohesion of the mix increases and self-weight of the mix reduces, thus, resulting in reducing of the self-leveling properties of the cellular concrete (Nambiar and Ramamurthy, 2006). There are two main properties that describe fresh state of the LCC: stability and consistency.

2.3.1.1 Stability

Khayat and Assaad (2002) defined stability as a state that is required to ensure the presence of an adequate air void system and maintain it in a stable state until the time of hardening in Self-Consolidating Concrete (SCC).

Factors affecting mix stability are the following: (Brady, Jones, and Watts, 2001; Jones, Ozlutas and Zheng, 2016)

- Environmental conditions (wind, evaporation, temperature, vibration)
- Materials used (quality and volume of foam)
- Quality of production (mixing and placing processes)

It was stated by a number of researchers (McGovern, 2000; Aldridge, 2005; Jones and McCarthy, 2005b, 2006; Mohammad, 2011) that instability of LCC was a result of poor foam quality as well as the type of constituents used. However, in the case of instability at ultra-low densities (600 kg/m^3 and less), the stability of the mix has been observed to occur even in the absence of the above-mentioned factors (Ozlutas, 2015). The nature of stability or instability depends on the size of the bubbles in the bubble structure. The draining properties of LCC allow water to penetrate inside the material and if stays there, causing the increase in the bubbles inside the structure; thus, collapsing the foam. Meanwhile, the strength of bubbles decreases and cannot support the pressures. Figure 2-4 demonstrates typical instability issue.

Figure 2-4: Instability Issues with Ultra-Low Density LCC (Field Performance)

2.3.1.2 Consistency and Workability

Consistency and workability of cellular concrete are usually characterized by its flowability. The presence of air-voids in the fresh mix due to the addition of stable foam agents allows LCC to be placed easily. The lightweight concrete can be pumped through flexible hoses over a distance of 200 m. Furthermore, its flowability allows it to easily spread into complex forms. It settles into place without the use of compaction equipment as it is self-consolidating material. This makes it an excellent candidate for pipe bedding, and for fill around utilities or not easily accessible areas. Since it flows so easily, forms usually have to be lined with plastic to prevent seepage. Also, the surface of LCC pours cannot be sloped greater than 1 degree due to its low viscosity (Taylor et al., 2016). Figure 2-5 shows a typical placement of LCC by flexible hose.

Figure 2-5: Lightweight Cellular Concrete being Placed with a Flexible Hose (Taylor et al., 2016)

2.3.1.3 Compatibility

According to Amran, Farzadnia, and Ali (2015), the compatibility of LCC is referred to as a condition of strong interaction between the mix design and its constituent parts, in particular between chemical admixtures and the foam agent. Thus, at the areas where the mixture constituents fail to interact, the compatibility of foam mortar decreases. In addition, segregation challenges may occur when there is no interaction between the surfactant and plasticizers (Brady, Jones and Watts, 2001).

2.3.2 **Hardened State**

Hardened state is characterized by mechanical, physical, durability and functional properties of the cellular concrete. These properties include compressive, flexural and tensile strength,

modulus of elasticity, porosity and permeability, drying shrinkage, freeze-thaw resistance, and Poisson's ratio.

2.3.2.1 Compressive Strength

The compressive strength represents the capacity of a material to resist loads due to compression. LCC has considerably lower range of densities (from 250 kg/m^3 to 1800 kg/m^3) than conventional concrete, thus lower compressive strength (Table 2-1). In general, compressive strength depends not only on density, but also on number of parameters such as rate of foam agent, w/c ratio, sand particle type, the curing method, cement/sand ratio, and characteristics of additional ingredients and their distribution (Valore, 1954b; Deijk, 1919; Valore, 1954a).

Table 2-1: Typical Properties of LCC Based on British Concrete Association (BCA, 1994)

Dry Density (kg/m^3)	Compressive Strength (MPa)	Modulus of Elasticity (MPa)	Thermal Conductivity (3% moisture) (W/mK)	Drying Shrinkage (%)
400	0.5-1.0	800-1000	0.10	0.30-0.35
600	1.0-1.5	1000-1500	0.11	0.22-0.25
800	2.0-2.5	2000-2500	0.17-0.23	0.2-0.22
1000	2.5-3.0	2500-3000	0.23-0.30	0.15-0.18
1200	4.5-5.5	3500-4000	0.38-0.42	0.09-0.11
1400	6.0-8.0	5000-6000	0.5-0.55	0.07-0.09
1600	7.5-10	10 000-12	0.62-0.66	0.06-0.07

2.3.2.2 Split Tensile Strength

Tensile strength is typically used as a concrete performance measure for pavements because it best simulates tensile stresses at the bottom of the concrete surface course as it is subjected to loading. These stresses are typically important in controlling structural design stresses (Pavement Interactive, 2018). A diametric compressive load is applied along the length of the cylinder until it fails. The test setup is shown in Figure 2-6. Because concrete is much weaker in tension than compression, the cylinder will typically fail due to horizontal tension and not vertical compression. The splitting tension test on regular concrete shows the value of 10% of its compressive strength (Raphael, 1984). For cellular concrete, it is still to be determined, but according to Amran, Farzadnia, and Ali (2015), the tensile strength is in the range between 20% and 40% of its compressive strength.

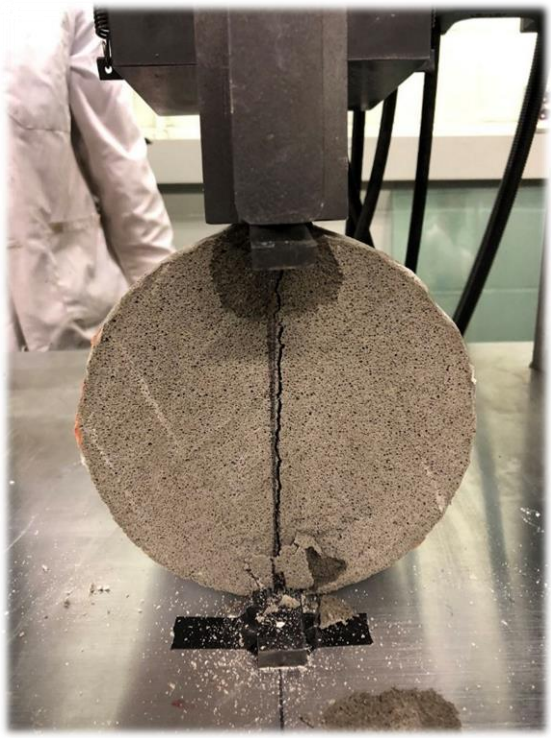

Figure 2-6: Splitting Tensile Strength Test Setup

2.3.2.3 Modulus of Elasticity

The modulus of elasticity in pavement design represents how much the concrete will compress under load (TAC, 2013). The modulus of elasticity generally correlates with compressive strength of LCC. Conventional concrete has a modulus of elasticity of 14,000 to 41,000 MPa, depending on compressive strength and aggregate type. It is reported that E-value of LCC is four times lower than conventional concrete (Jones and McCarthy, 2005b). In cellular concrete, the modulus of elasticity is more related to its density. According to the studies, for range of dry density from 500 to 1600 kg/m^3, the modulus of elasticity typically falls between 1.0 and

12 kN/m^2 respectively (Brad, Jones and Watts, 2001). In addition, it was stated by Jones and McCarthy (2005b) that E-value is dependent on the composition of the mix, and may be altered by fly ash or sand addition. Table 2-2 presents the relationship between compressive strength, modulus of elasticity and density.

Table 2-2: Empirical Model for Cellular Concrete Modulus of Elasticity Determination (Amran, Farzadnia and Ali, 2015)

Equations	Annotations
$E = 33W^{1.5}(fc)^{0.5}$	Pauw's equation
$E = 0.99\ (fc)^{0.67}$	Fly ash utilized as fine aggregate
$E = 0.42\ (fc)^{1.18}$	Sand is utilized as fine aggregate
$E = 5.31$ x W-853	Density ranges from 200 to 800 kg/m^3
$E = 6326(\gamma_{con})^{1.5}\ (fc)^{0.5}$	γ_{con} = unit weight of concrete fc =compressive strength of concrete where average Poisson's ratio=0.2, and using polymer foam agent
$E = 57,000\ (fc)^{0.5}$	Density of conventional concrete limited between 2200 and 2400 kg/m^3 substituting with 80 kg/m^3 for steel
$E = 9.10\ (fc)^{0.33}$	fc = compressive strength of concrete
$E = 1.70$ x 10^{-6}p$^2(fc)^{0.33}$	p = plastic density (kg/m^3)

2.3.2.4 Drying Shrinkage

Drying shrinkage is a damaging process to concrete that is caused by the loss of absorbed water from the material. Due to high total porosity (40-80%) drying shrinkage is of high significance in lightweight cellular concrete. The main reasons that intensify shrinkage include pore size decrease as well as a growing number of small-sized pores. Drying shrinkage of LCC where cement is the only binder is notably higher than the one manufactured with lime or lime and cement. Air-cured specimens have very high drying shrinkage potential. On the contrary, moist-cured cement and sand mixes demonstrate drying shrinkage values ranging from 0.06% to over 3.0% when dried at normal temperature, the lowest numbers are correlated with higher densities and higher percentage of sand. The time dependence of shrinkage is inclined by the properties of material, size of specimen and shrinkage climate. In addition to these factors, shrinkage value varies according to the initial moisture content. In the range of higher moisture content (>20% by volume), comparatively insignificant shrinkage takes place accompanied by loss of

moisture, which, in its turn, can be explained by the presence of a large amount of big pores which do not facilitate shrinkage (Darshan, 2016).

2.3.2.5 Poisson's Ratio

Poisson's ratio shows the lateral to axial strain relationship for a material under the load. Its value is obtained using the strains resulting from uniaxial stress only. Poisson's ratio is one of the input parameters for MEPDG (TAC, 2013). The typical range of Poisson's ratio for cellular concrete with densities of 1000 kg/m^3 to 1400 kg/m^3 is 0.13 to 0.16 and 0.18 to 0.19 respectively (Lee et al., 2009). Neville (2011) reported that the Poisson ratio for normal weight concrete is 0.15 to 0.22. Study by Tiwari et al., (2017) found Poisson ratio for LCC to range between 0.2 to 0.3 for LCC densities between 230 kg/m^3 to 800 kg/m^3.

2.3.2.6 Porosity and Permeability

Porosity is a measure of the voids in cellular concrete in comparison to the total volume. Porosity can affect the other material properties such as compressive strength, flexural strength, and durability (Amran, Farzadnia and Ali, 2015). However, Amran, Farzadnia, and Ali (2015) are reporting that the permeability and the degree of fluid flow through the concrete matrix were not significantly related to the total porosity, but to larger capillary pores. The porosity of LCC concrete allows the aggressive fluids to penetrate inside the matrix of the concrete in the hardened stage. Porosity of the hardened concrete may be affected by mix design compositions, foam agents, w/c ratio and the curing type. The porosity depends on degree of infusion characteristics such as water absorption, sorption, and permeability.

According to Sabir, Wild and O'Farrell (1997), permeability is defined as a measure of the water flow under pressure in a saturated porous medium. Permeability of the cellular concrete has a significant correlation with the water absorption of the material. Water absorption of the cellular concrete is twice conventional concrete at similar water to binder ratio. Moreover, permeability may be affected by the inclusion of aggregates or mineral admixtures and entrained air in the cement paste (Amran, Farzadnia and Ali, 2015).

2.3.2.7 Freeze-Thaw Resistance

Lower density LCC has been observed to have good freeze-thaw resistance due to the voids restraining the expansion forces from frozen water (Brady, Jones and Watts, 2001). Freeze-thaw characteristic of LCC is dependent on its initial depth of penetration, absorption and absorption rate (Jones, 2001).

2.3.2.8 Thermal Insulation and Conductivity

Another benefit of LCC which stands out against the other materials is its thermal properties. The air entrapped within the concrete acts as an insulator, so heat does not easily transfer

through. This makes LCC desirable as an insulation in buildings, or in tank bases to prevent heat damage to liners (Taylor et al., 2016). Moisture content, density and components of the material account for its thermal conductivity. Density is the key factor in thermal conductivity, as the way of curing the product (moist-curing or autoclaving) is of no importance here. The number of pores and their arrangement are essential for thermal insulation as well. Smaller pores have been found to facilitate better insulation (Darshan, 2016). Concrete is inert and fireproof and does not easily conduct sound, which further suggests it would be a good material for insulation.

A drawback for LCC of being a good insulator is frost heave. Because of that, there can be differential heating and cooling between the cellular concrete and the surrounding materials. If the LCC is used in pavement subgrade, water can seep through the highly porous matrix and pool in areas. Differential cooling in the wintertime can cause ice to form, which expands and causes upheaval that can damage overlying pavements and structures. To mitigate this risk, LCC forms should be sloped downward to the sides and extended out past the overlying road or structure so water cannot pool at the base of the concrete (Maher and Hagan, 2016).

2.3.2.9 Buoyancy Forces

Density of LCC can be less than half the density of water, so if the concrete is submerged there will be buoyancy forces. For an application such as a river embankment fill material, this could be a major problem: if river banks rise, buoyancy forces can push the concrete upwards causing upheaval and failure of the overlying pavements and structures (Friesen et al., 2012).

2.4 Challenges

Number of advantages and disadvantages were discussed in this Chapter. Challenges, associated with LCC are summarized as follows:

- LCC has high potential of drying shrinkage because of the significant amount of cement in its composition (up to 80 % of cement). According to Ramamurthy (2009), LCC can be 10 times more susceptible to drying shrinkage than conventional concrete.
- Instability issues could be a significant problem, especially at the ultra-low densities of LCC during construction process.
- Initial cost might be higher than for similar lightweight materials or for Granular materials, if measuring them m^3 to m^3. However, in most projects less m^3 of LCC is needed to obtain the same performance.
- Since LCC has good flowability, it may be challenging to place it on the slope surfaces. The technique of “lifts” may be used, when LCC is being placed by levels in steps. Although, this method requires additional framework.

- Another issue with LCC material can be its seepage through the underlying layers when it is placed over the open graded layers. Additional protective layers such as polyethylene sheets may be used to prevent this problem.
- Groundwater seepage control of the excavations, where LCC will be placed, is required. This needs to be done to prevent floating of the material, as LCC density for the case studies was 475 kg /m^3, which is less than water density (1000 kg /m^3).

2.5 Sustainability

Sustainable development according to the World Commission on Environment and Development (WCED, 1987) is defined as: "Development that meets the needs of the present without compromising the ability of future generations to meet their own needs".

The potential sustainability benefits of using LCC are outlined below:

- At low densities, it can contain 80 -90% voids which means less virgin material usage and waste produced (Ozlutas, 2015).
- Reduction in the use of non – renewable natural resource by eliminating coarse aggregates, and fine aggregates at densities below 600 kg/m^3 (BCA, 1994).
- It makes use of industry by-product such as slag and fly ash thereby reducing the amount of waste disposed (Dolton et al., 2016; Jones et al., 2012; Awang et al., 2014). Fly ash can also be used to replace Portland Cement up to 75% in lower density LCC, this has the advantage of reducing embodied CO2 (eCO2).
- No need for compaction as it flows freely, therefore noise pollution reduction during construction and less energy consumed as compaction is eliminated (Jones and McCarthy, 2005a).
- Not only has it great constructability as the material can be installed very quickly, but also can be placed during winter time with some protective measures and during the light rain (Maher and Hagan, 2016).
- LCC can be easily excavated and removed as it has low strength.
- It can be recycled and used for producing more cellular concrete (Jones et al., 2012).
- LCC has been shown to have good freeze-thaw resistance (Ramamurthy, Nambiar and Ranjani, 2009), fire resistance, sound absorption, and superior thermal insulating properties which improve with lower plastic densities (Wei et al., 2013; Jones and McCarthy, 2005a).
- Due to its high strength-to-weight ratio, there is typically less material required for fill operations, which means less machinery is required during manufacturing and construction, leading to less energy use, less greenhouse gas emissions, and less noise pollution (Dolton et al., 2016).

2.6 Applications

Lightweight fill materials are increasingly being used in civil engineering applications such as roadway base layers, embankment fill material, grout for tunnels and pipes, soil stabilization, fill for abandoned mines or other types of void fill, landslip repair, arrestor material at the end of airport runways, sound-dampening walls, fireproof insulation, and retaining wall backfill (Maher and Hagan, 2016; Horpibulsuk et al., 2014). The air bubble structure of LCC is exceptional at absorbing energy, so there have been successful uses of this material in military ranges, as rockfall protection, and in airports as the safety barrier in order to safely slow down planes and jets if they were to overshoot their runways (Taylor et al., 2016). Amran, Farzadnai, and Ali (2015) report a significant interest in LCC in North America, and in Canada in particular, not only because this material has a wide range of applications but also because of the increased prices for the other lightweight building materials. The annual market size of cellular concrete is estimated to be about 250,000 – 300,000 m^3 in United Kingdom including massive mine stabilization project. In Western Canada, the market size of LCC is about 50,000 m^3 and it is actively growing. North Koreans mostly use cellular concrete in floor heating systems with the total market for this country as 250,000 m^3. In order to reduce the effect of earthquakes and to mitigate the effect from temperature changes, cellular concrete is being used in the Middle East. It can be used as a great thermal insulator for those cases (Amran, Farzadnia and Ali, 2015).

LCC has been used in more than 50 countries. Oginni (2015) presented Figure 2-7, indicating use of cellular concrete technology globally. Asia and Europe alone accounted for 83% of the use of cellular concrete technology economy worldwide.

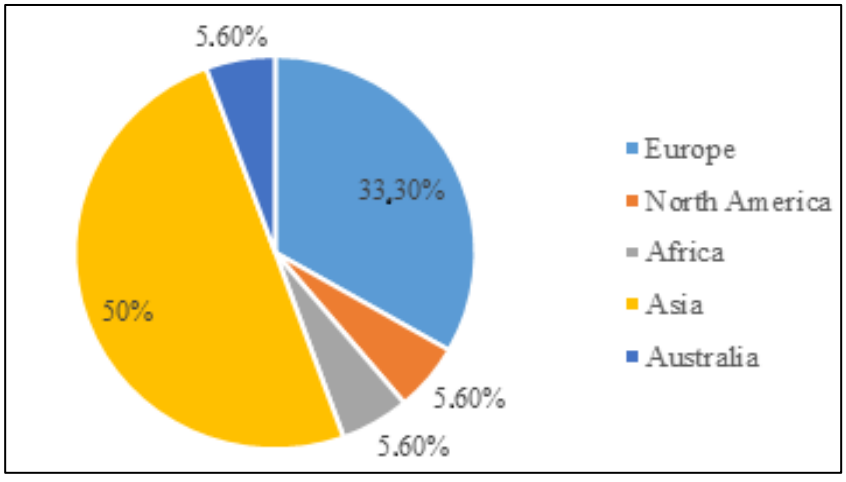

Figure 2-7: Global Use of Cellular Concrete (Oginni, 2015)

The main intent of lightweight fill materials is an alternative construction material to significantly reduce the weight of fills, thereby mitigating excessive settlements and bearing failures. This can subsequently result in more economic designs for structures such as retaining walls and base layer of roadways. The summary of the typical usage of the cellular concrete based on its density is studied and presented in Table 2-3. Moreover, density is potentially easier to control than compressive strength while placing the LCC.

Table 2-3: Summary of Cellular Concrete Applications Based on Density (Sari and Sani, 2017)

Density (kg/m^3)	Application
300-600	Replacement of existing soil, soil stabilization, raft foundation.
500-600	Currently being used to stabilize a redundant, geotechnical rehabilitation and soil settlement. Road construction.
600-800	Widely used in void filling, as an alternative to granular fill. Some such applications include filling of old sewer pipes, wells, basement, and subways.
800-900	Primarily used in production of blocks and other non-load bearing building element such as balcony railing, partitions, parapets, etc.
1100-1400	Used in prefabrication and cast-in-place wall, either load bearing or non-load bearing and floor screeds.
1100-1500	Housing applications.
1600-1800	Recommended for slabs and other load-bearing building element where higher strength required.

2.7 Applications in Pavement Engineering

Various lightweight fill materials including LCC have been developed in recent years for usage in various civil engineering applications (Arulrajah et al., 2015). It has potential success in being used as a material for structural purposes, stabilization of weak soils, base layer of sandwich solutions for foundation slabs, industrial floor and highway as well as subway engineering applications (Kadela, Kozlowski and Kukielka, 2017).

Maher and Hagan (2016) state that the biggest issue in constructing the highways and roads over peat, organics or soft soil deposits is continual and long-term settlements that are hard to address. Full depth reconstruction requires long-term closures of the damaged pavement section. Moreover, it is usually expensive and not an efficient way of solving the problem. According to Kadela, Kozlowski, and Kukielka (2017), areas with difficult geotechnical conditions are characterized as weak soils, including grounds containing layers of organic layers. Factors, influencing decision-making processes of choosing the proper method for

dealing with those issues include geological substrate system, size of loads acting on subsoil, excessive moisture of soil, technological capabilities and costs of using the technology. Kadela, Kozlowski, and Kukielka (2017) introduced several methods of dealing with those weak soils and LCC as a potential solution to this issue was studied.

Maher and Hagan (2016) stated that using cellular concrete in the areas with weak soils allows pavement to be "floated" over the subgrade as the density of this material is a quarter of that of conventional granular fill and it is a less expensive solution than traditional lightweight materials such as polystyrene. In terms of ability of the lightweight cellular concrete to bear the loads, Kadela, Kozlowski, and Kukielka have presented the results of numerical simulations that proves that using cellular concrete as a subbase layer is potentially possible in terms of bearing the loads. The same study has shown that the tensile stress in the lower zone of the subbase layer is lower than the flexural strength of LCC that was tested.

2.8 Summary of Literature Review and Research Gaps

Lightweight Cellular Concrete offers potential construction, performance, sustainable and cost benefits when used in a pavement structure. As an alternative roadbed support over weak soils, LCC has been installed as pavement subbase material to provide more stable and stronger foundations. It has been placed in a few pavement sections across Canada and preliminary information shows that it can improve pavement performance. However, there is a lack of integrated field and laboratory evaluation, adequate information, and practices of using LCC as pavement subbase layer. There is a need to investigate the in-situ performance as a material incorporated into the pavement structure.

The overall purpose of this project is to summarize the information about the performance of the pavement sections with LCC in its structure. The laboratory tests are concentrated on mechanical properties and the possible correlation between parameters, characterizing cellular concrete in terms of density, UCS, and modulus of elasticity.

Another aim of this research is to predict the LCC performance for a given sections and compare it to the typical pavement structures in terms of failure criteria.

CHAPTER 3

3 FIELD PERFORMANCE REVIEW

This Chapter describes five road sections with installed Lightweight Cellular Concrete (LCC) layer as a subbase. All the available information was compiled in a table and analyzed at the end of the Chapter. Similar features of the road sections, as well as challenges during construction and recommendations for the future construction of similar pavement, are discussed in this Chapter. In addition, methodology for the thesis is described in this Chapter (Figure 3-1).

3.1 Methodology

For analyzing the construction experience of using LCC as a subbase material, past projects (case studies) were studied. As a first step of collecting the data, published papers on the past projects where LCC was installed as a subbase layer were studied. After that, technical reports were analyzed and visual inspections on the road sections were completed. All of the available information from the road sections was compiled and analyzed concluding in similarities and/or differences in the performance.

After analyzing the data from the past projects, the next step was to predict performance of the installed LCC sections in the future. Chapter 4 aimed to predict the performance of the road sections located in Ontario in terms of fatigue cracking and rutting resistance. In addition, bearing capacity of the road sections was determined. These parameters were discussed under the failure criteria analysis. Furthermore, the comparison between LCC and Granular B subbase materials that were installed on the same road sections was completed and discussed.

Knowing the current condition of the LCC road sections that were reconstructed in the past as well as having an idea of the predicted performance of the sections in the future, it is crucial to understand the mechanical properties of LCC that are currently being used in construction. In Chapter 5, mechanical properties of the in-situ cast samples will be determined and compared to the typical values in literature. In addition, the relationship between the mechanical properties of LCC will be discussed.

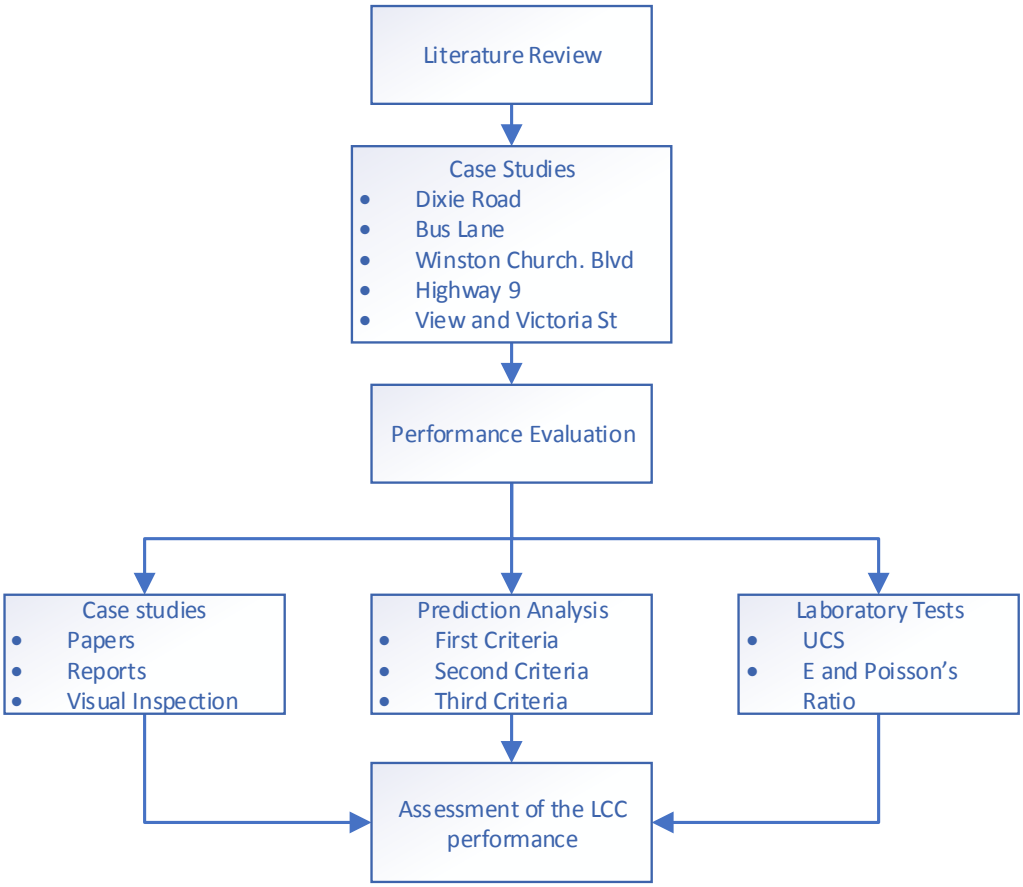

Figure 3-1: Overview of Research Methodology

3.2 Case Studies

LCC may be used in many applications in infrastructure projects. Currently, there are not many companies who produce and provide cellular concrete solutions. There are several cases when LCC was installed into roadway sections and infrastructure applications in Canada. The scope of this project is to study the LCC as a subbase layer.

Five road sections that were constructed using LCC as a subbase layer were investigated, including Dixie Road, Winston Churchill Boulevard, Highway 9, Brentwood Light Rail Transit (LRT) Bus-Lane and View and Vancouver Streets. All five sections have similar pavement structures, including an asphalt concrete surface layer, an unbound granular base layer, a lightweight cellular concrete subbase layer, and subgrade soil. The pavement surface distresses were determined by following ASTM D6433, which classifies nineteen types of pavement distresses. These distresses such as alligator cracking, bleeding, corrugation, longitudinal and transverse cracking, and rutting were inspected. The inspections were conducted manually

instead of using automated data collection vehicles. The results of the field inspections are described in the following sections.

3.2.1 Dixie Road. Region of Peel, Caledon, Ontario, Canada

3.2.1.1 Background

The Region of Peel reconstructed a 120-metre section of rural highway in 2009. The main issue, within the section, was ongoing settlement for a number of years. The proposed solution was required to be environmentally friendly and to minimize the impact on the adjoining wetlands. Instead of removing and replacing the existing embankment with granular material, the Region chose to use lightweight cellular concrete as an alternative. Traditional reconstruction would have required considerable dewatering, extensive peat removal, the erection of sheet piling and then replacing peat with granular materials. Figure 3-2 demonstrates the location of the road.

Figure 3-2: Road Section Location (Google maps, 2018)

A geotechnical investigation was completed before reconstruction of the road in 2009. This investigation included pavement cores and boreholes throughout the settlement area, resulting in the following conclusions:

- Thickness of the asphalt layer ranged from 150 mm to 280 mm
- Granular base/subbase was at the depth from 1.4 to 1.8 m
- Peat/marl deposits were located from the depth of 2.1 m up to 5.4 m. with $M_r = 17$ MPa

After the geotechnical investigation was done by a contractor. Full excavation of the weak soils, followed by backfilling with granular material was suggested. The pavement structure to support 500,000 cumulative ESALs was recommended as follows:

- Removal of existing material - 5.2 m
- Hot Mix Asphalt - 140 mm
- Granular A Base Course - 150 mm
- Granular B Type I Subbase - 400 mm

Instead of removing and replacing the embankment to a depth of 5.2 m, the Region chose the following pavement structure:

- Hot Mix Asphalt - 140 mm
- Granular A Base Course - 150 mm
- LCC CEMATRIX CMEF-475 (CEMATRIX Manufactured Engineering Fill) - 650 mm

The typical cross section for the cellular concrete section is presented in Figure 3-3.

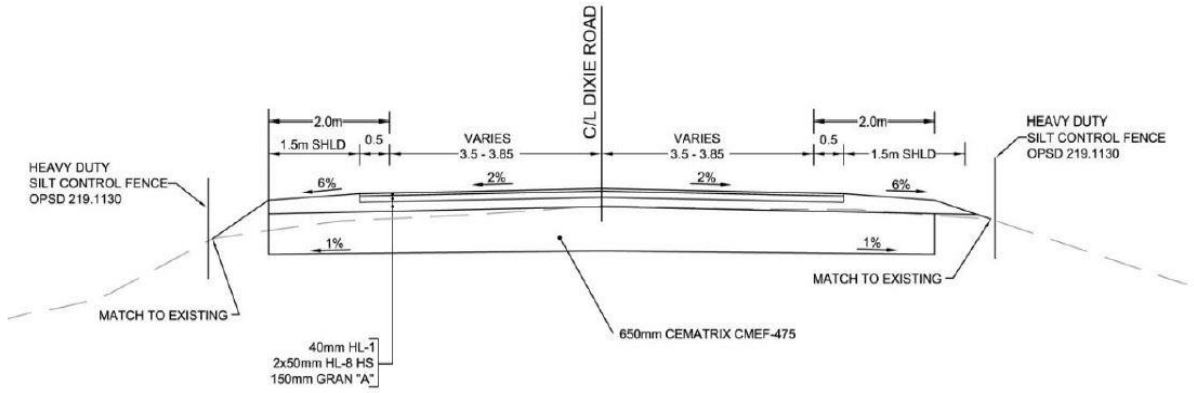

Figure 3-3: Typical Cellular Cross Section (Griffiths and Popik, 2013)

Cellular concrete was produced and placed on site by CEMATRIX Company with the dry-mix production units. The construction process is shown in Figure 3-4.

Figure 3-4: Construction Process of Dixie Road, Region of Peel, Caledon, Ontario, Canada (CEMATRIX)

3.2.1.2 Field Investigation

Griffiths and Popik (2013) investigated the in-place performance in 2013. The evaluation of the section included the following:

- Visual condition survey of the existing pavement surface
- Ground Penetrating Radar (GPR) survey with various transverse scans to provide layer thicknesses and subsurface images of the pavement utilizing the CEMATRIX LCC
- Falling Weight Deflectometer (FWD) testing to determine the structural capacity of the lightweight cellular concrete section in comparison with the adjacent pavement

Visual Condition Survey

The visual pavement condition survey of the site was completed on June 4, 2013, and concluded that pavement section was in good condition. In total, three slight longitudinal cracks and one moderate pavement distortion/heave were observed in the area. Figure 3-5 shows the cracks. The longitudinal cracks were located in the northbound lane, approximately at the midpoint of the site.

Longitudinal Cracking (centreline)

Transverse Cracking

Minor crack

Transverse Cracking

Figure 3-5: Condition of Dixie Road, Region of Peel, Caledon, Ontario, Canada

All three cracks were found to be close to the centreline, with a slight meander into the outer wheel-path. The pavement distortion/heave at the north transition extended for approximately 25 m and appeared to be worse in the southbound lane, than in the northbound direction. The distress appeared to be caused by a heave in the area marked at the end of the LCC material. The adjacent pavement sections were also investigated, and it appears to be in excellent condition without any distresses. In general, the condition of the section is performing adequately after three years of construction.

It was also observed that LCC material was exposed at the SB shoulder rounding. It was observed that part of the gravel, which was intended to cover and protect the LCC from weather, was eroded into the ditch. Thus, the LCC layer was easily broken from the exposed edge.

A. Ground Penetrating Radar

As part of this evaluation, a Ground Penetrating Radar (GPR) survey was completed. GPR is a non-destructive device that uses a radar pulse to produce subsurface images. Ground Penetrating Radar equipment is shown in Figure 3-6.

The GPR survey was completed in order to identify the thicknesses of the pavement layers and the border with the adjacent road sections. More comprehensive GPR surveying was completed at the areas containing longitudinal cracking. The GPR data was collected by summarizing results obtained from 3 cycles of measurement for each line:

1. Using SmartCart, equipped with a NOGGIN 250 MHz GPR sensor
2. Using SmartCart, equipped with a NOGGIN 500 MHz GPR sensor
3. Using SmartCart, equipped with a NOGGIN 1000 MHz GPR sensor

Figure 3-6: Ground Penetrating Radar Equipment

Griffiths and Popik (2013) reported that thicknesses of the pavement layers varied (some of which were within the normal range and some were not). For example, Table 3-1 shows a part of the report for lane №10 (L10):

Table 3-1: Comparison of Pavement Structures

Layers	Designed, mm	GPR reading (range), mm
Asphalt	140	126-178
Granular Base	150	68-235
LCC	650	Vary because of the not flat underlying subgrade

Longitudinal and transverse images of the lanes were also obtained (Figures 3-7, 3-8).

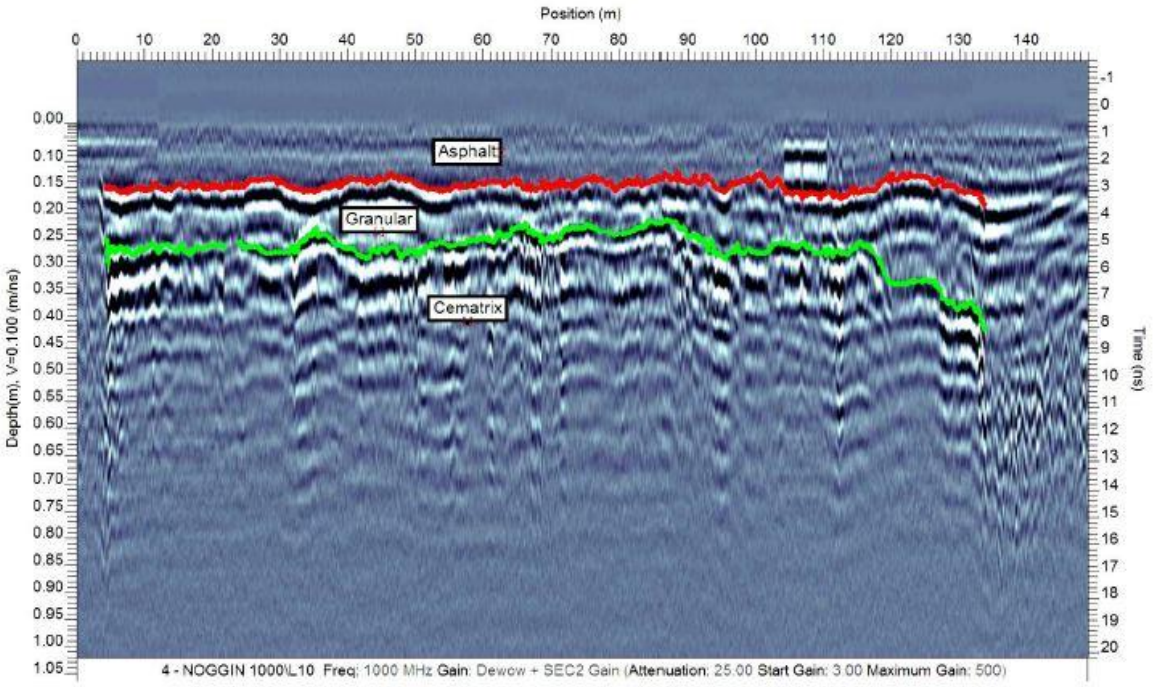

Figure 3-7: GPR Longitudinal Image of Southbound Lane, L10 (Griffiths and Popik, 2013)

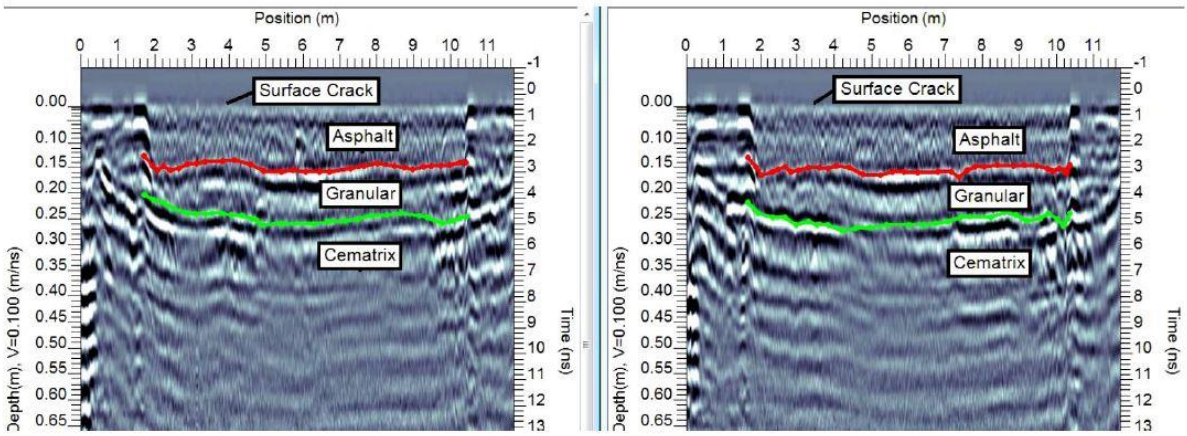

Figure 3-8: GPR Transverse Images at Longitudinal Crack Locations, L4, and L5 (Griffiths and Popik, 2013)

B. Falling Weight Deflectometer

Pavement load/deflection testing was completed on July 30, 2013, and included 54 tests. The Dynatest Falling Weight Deflectometer (FWD) was used for the structural evaluation of this pavement section. On the traditional road section, from the both sides of the LCC section, FWD testing was completed every 5 m in southbound and northbound directions. For the transition areas, between LCC and traditional section, FWD testing was completed on 2 m intervals for a length of 10 m. Each test included 4 drops, with the first drop being a seating load, and the following three loads at roughly 30, 40 and 75 kN. The testing equipment is shown in Figure 3-9. Full FWD report is presented in Appendix I.

Figure 3-9: FWD Truck and Trailer (Griffiths and Popik, 2013)

The collected FWD data was analyzed based on the pavement thickness measured by the GPR survey. For the purposes of the FWD analysis within the Lightweight Cellular Concrete section, the LCC layer was assumed to be part of the pavement structure. Two parameters were determined: the composite elastic pavement modulus and the structural coefficient. The composite elastic pavement modulus of LCC section ranged from 714 to 737 MPa, which is higher than the adjacent section (514 to 670 MPa). This resulted in increasing of the composite pavement structural number of LCC section, which ranges from 175 to 224 mm while the adjacent section range from 128 to 154 mm.

The structural coefficient of the LCC material was determined by the analysis of FWD data. The structural coefficients of the asphalt and Granular base layers used in the analysis were 0.38 and 0.12 respectively (Griffiths and Popik, 2013). In comparing the overall strength of the LCC section, the composite elastic pavement modulus of the pavement structure incorporating the LCC material was found to be stronger, than the adjacent conventional pavement structures (Figure 3-10).

The calculated structural number (SN) for each layer was added together and subtracted from the SNEff at each FWD test location. The resulting SN for the LCC layer was divided by the layer thickness of 650 mm to obtain the equivalent AASHTO structural coefficient for the LCC material. The averaged back-calculated structural coefficient for the LCC material used on this site is approximately 0.2, after removing outliers that were more than one standard deviation of the average. In conclusion, following the AASHTO flexible pavement design methodology for designing a flexible pavement utilizing the CEMATRIX LCC-475 (with a density of 475 kg/m^3), a structural coefficient of 0.2 should be used. Structural coefficient was obtained after the road had been in use for four years, thus, some adjustments may be applied to the structural coefficient. Similar tests may be conducted in the future on the newly constructed pavements in order to determine structural coefficient soon after construction.

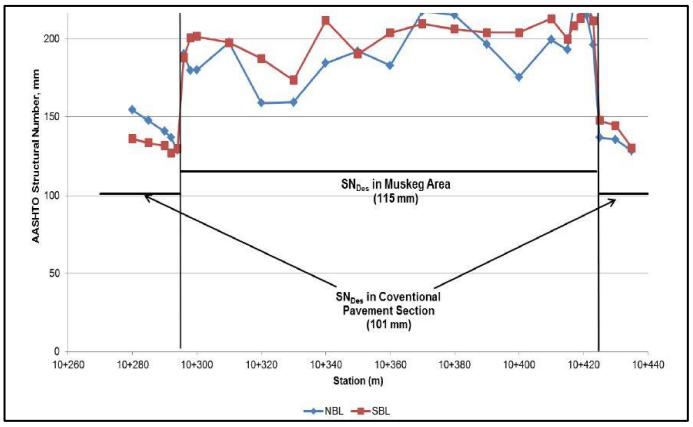

Figure 3-10: Structural Number Comparison Plot (Griffiths and Popik, 2013)

3.2.1.3 Findings and Discussion

1. In general, the pavement structure on Dixie Road appeared to be in good condition, with few distresses. With the LCC section in service for roughly three years, it is encouraging to see that the condition of the roadway in this section continued to perform similarly to the pavements adjacent on either side of the LCC section.
2. The overall average asphalt thickness along the whole road section is close to the designed number – 148 mm vs 140 mm. The thickness of the Granular base is not consistent and in some places, it is thinner than the design requirement of 150 mm. The lowest thickness of the Granular base is 68 mm which was found in the place where longitudinal cracks were observed by visual survey.
3. It was also observed that the top of the LCC layer was not flat at the border with the adjacent road section. It was observed on the longitudinal image of the GPR survey. Because of that, the granular layer was detected as thick as 235 mm instead of designed 150 mm. Griffiths and Popik (2013) linked this information with the fact that some distortions on the pavement surface in this area were observed as consequences of some ground movement continued after construction.
4. In order to access those distresses and its cause, a detailed forensic investigation was recommended.
5. It can be noticed that on the GPR transverse images that pavement layers were shown as a bowl shape, with the sides of the layers going up. Griffiths and Popik (2013) reported that this is a result of the top surface, which was constructed with a crossfall but was shown on the image as a flat line. If these images were adjusted to include the surface crossfall of the pavement and shoulders, then the top of LCC layer would have shown a relative flat surface.
6. The construction of the LCC embankment should be completed in lifts, with suitable layer thicknesses to optimize strength of the material, with the practical construction of the embankment. It is recommended that the individual lift thickness do not exceed 300 mm. Furthermore, the design of each lift should be such that the edges of the upper lift are offset by a minimum of 500 mm inward from the edge of the lower lift. The LCC layer should be constructed with a pyramid shape, with the top lift constructed 0.5 m beyond the edge of the travel lane. The staggering of the various lifts of the LCC embankment will allow for easier grading of the embankment slopes while maintaining adequate coverage of the LCC material at all times.
7. The top lift should also be constructed with a minimum 1 percent cross-fall, so that subsurface drainage is maintained at the top of the LCC material toward the outside ditches. Any imperfections in the transverse profile of this layer could create a ‘bath-tub’ situation, which would trap water at this layer interface. This could affect the performance in the Granular base material placed on top of the LCC layer. The embankment slopes should be covered using Granular base type material, with the

embankment slope designed to minimize erosion of the material that could potentially expose the LCC. Transitions at each end of the LCC embankment should also be carefully designed to provide a smooth transition and minimize any abrupt heaves with the adjacent earth embankments. It is critical that frost susceptible material is not used to construct the transition areas. Furthermore, the design of these transitions will need to ensure that they are constructible while meeting the foundation requirements for embankment stability.

3.2.2 Brentwood Light Rail Transit (LRT) Bus-Lane. Calgary, Alberta, Canada

The Brentwood bus-lane in Calgary was experiencing heavy loading due to the single rear axles of city buses. The bus lane had traffic volumes of up to 100 buses per hour and had frost-heaved substantially and became virtually impossible to drive on. The subbase of the road was composed of saturated silty deposits, over 30 m in depth. The subgrade soil had a California Bearing Ratio (CBR) of 0.8%. In 2000, the road was completely reconstructed with the following structure:

- 125 mm of asphalt
- 150 mm of Granular base course
- 200 mm of CEMATRIX CMRI-475 Insulating Road Base
- 50 mm of drainage rock (with subdrains beneath the curb & gutter)
- Geotextile fabric

The location of the road section is presented in Figure 3-11.

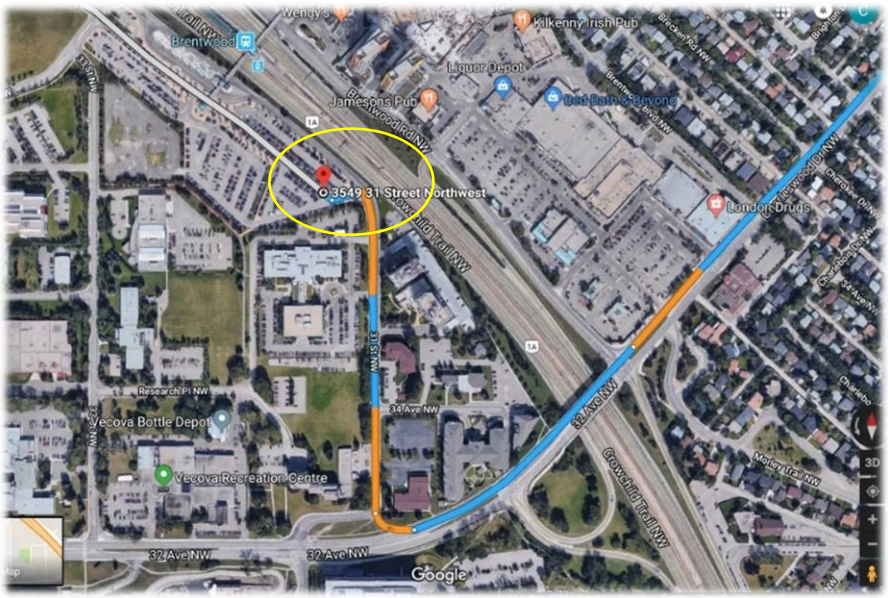

Figure 3-11: Site Location (Google Maps, 2018)

Figure 3-12 presents the reconstruction process of the bus-lane before and after pouring the LCC material.

(a) *(b)*

Figure 3-12: Bus Lane. (a) Reconstruction Process. Placing the LCC (CEMATRIX) (b) After Installing the LCC Layer (CEMATRIX)

Since construction, the road has experienced no frost heaving and required no additional remediation between 2000 and April 2018. A Benkelman Beam Deflection Test resulted in 0.012 inches (0.30 mm) of deflection, much less than the 0.035 inches (0.89 mm) allowed for such a road.

The performance of the LCC section in comparison to the adjacent conventional pavement structure is shown in Figures 3-13 and 3-14. The transition area between the LCC and non-LCC section is obvious and distresses at the conventional section were observed after the visual inspection in April 2018. The Lightweight Cellular Concrete section performed for a significant period of time (18 years) without any potholes and severe cracks. No maintenance was conducted to this section of the road during its service life.

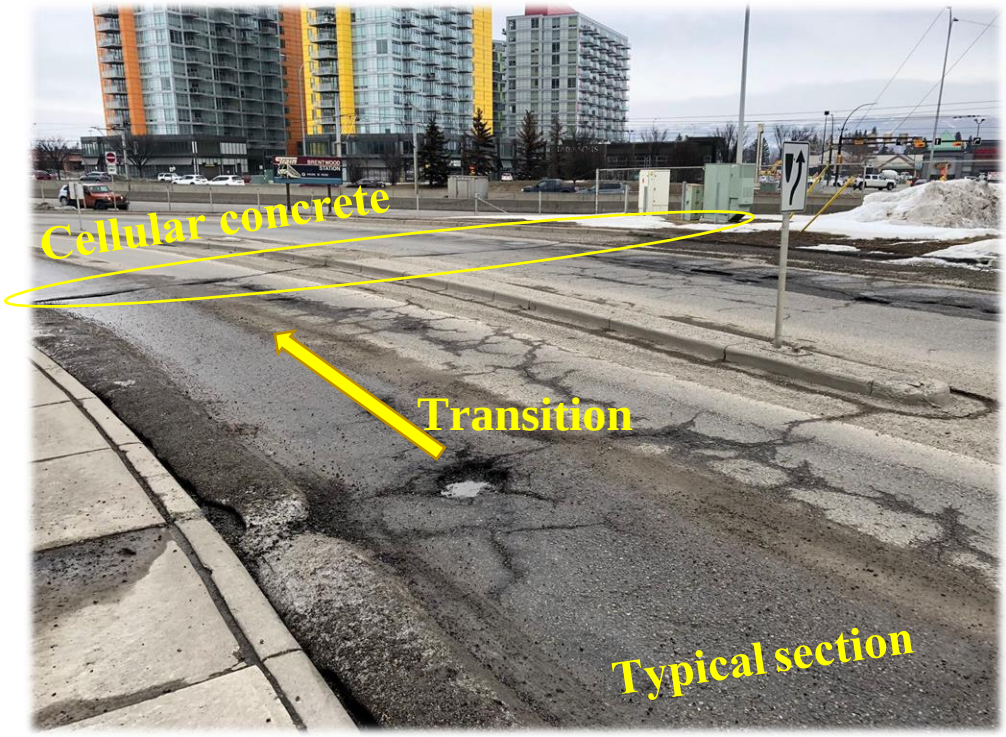

Figure 3-13: Pavement Distresses on the non-LCC section - 1(CEMATRIX, 2018)

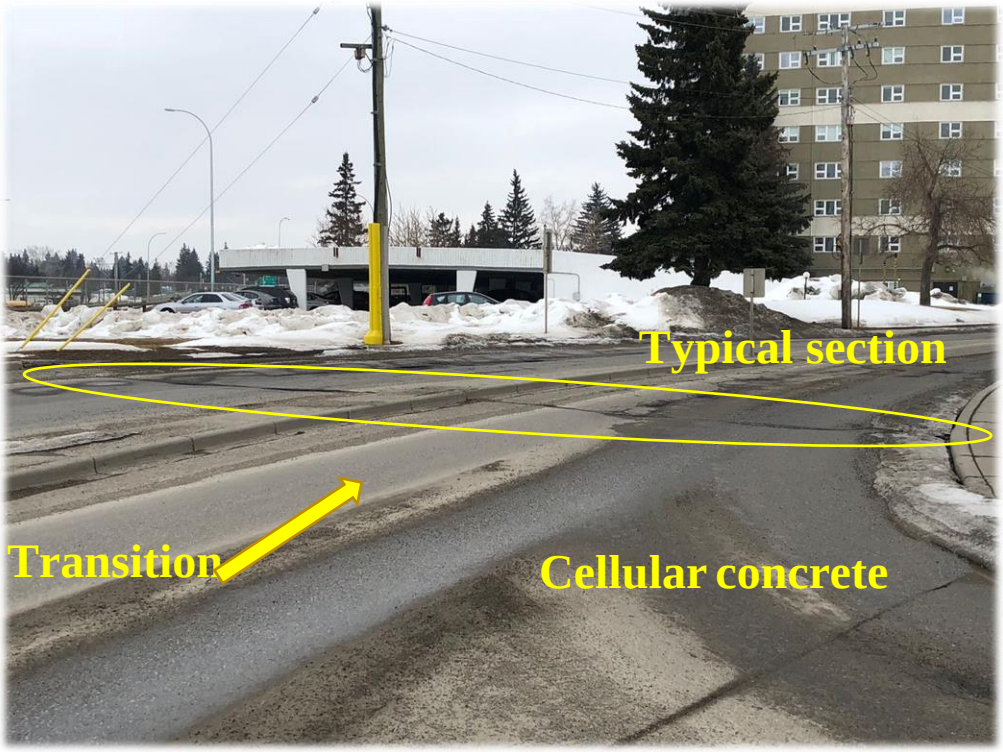

Figure 3-14: Pavement Distresses on the non-LCC section – 2 (CEMATRIX, 2018)

3.2.3 **Winston Churchill Boulevard. Brampton, Ontario, Canada**

The reconstruction of Winston Churchill Boulevard is similar to the Dixie Road project. It is a two-lane rural road. The project was completed in 2016. The location of the road section is presented in Figure 3-15.

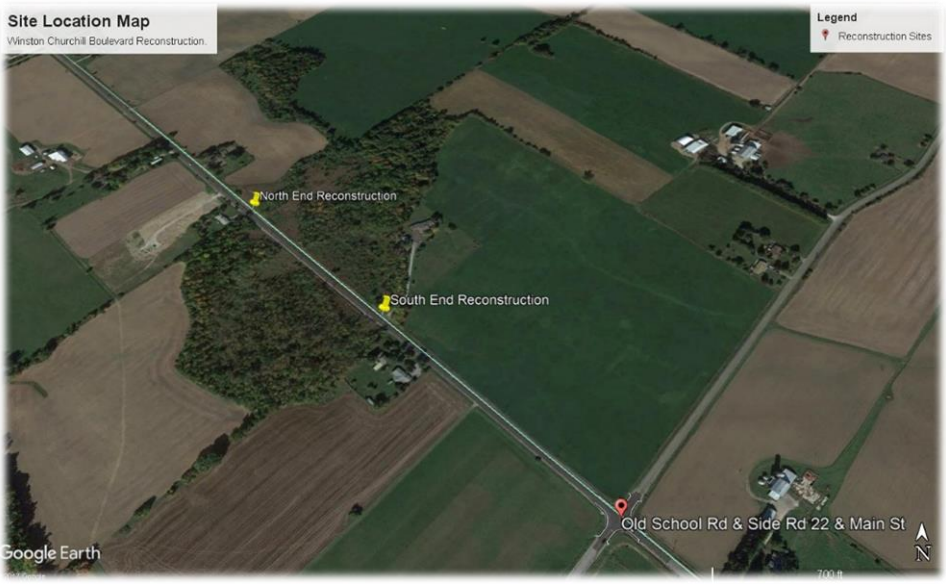

Figure 3-15: Location of the Road Section (Google Maps, 2018)

The pavement structure consists of the following layers:

- Asphalt concrete layer - 120 mm
- Granular A base layer - 240 mm
- Lightweight Cellular Concrete at the density of 475 kg/m^3 – 550 mm
- Existing subgrade – peat

The pavement structure that was installed on Winston Churchill Boulevard is shown in Figure 3-16.

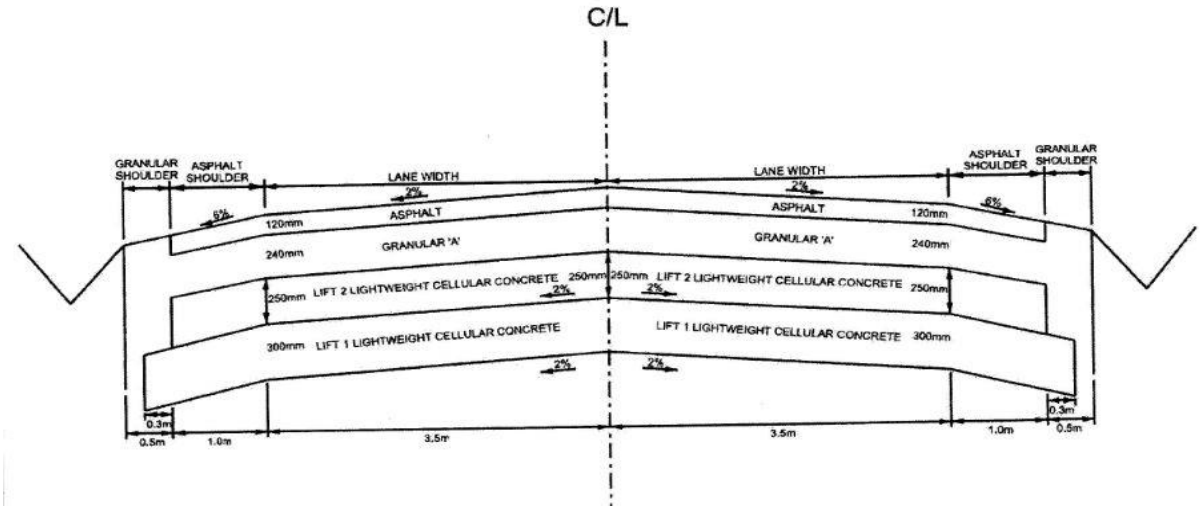

Figure 3-16: Pavement Structure. Winston Churchill Boulevard (CEMATRIX)

The field inspection found that the pavement remains in good condition after one year of construction. No severe cracks or rutting were found during the inspection (Figures 3-17 a, 3-17 b).

(a) *(b)*

Figure 3-17: Condition of Winston Churchill Boulevard, August 2017 (one year after construction). (a), (b) – Overall Condition of the Road

3.2.4 **Highway 9. Holland Marsh, Ontario, Canada**

The Highway 9 site is located north of Toronto. It is 1.5 km meters west from Highway 400. The location of the problematic area on Highway 9 is presented in Figure 3-18.

Figure 3-18: Highway 9 Site Location (Google Maps, 2018)

The construction project on Highway 9 aimed to overcome a weak soil problem. The soil in this area included thick organic deposits, which are challenging for pavement design. According to the geotechnical investigation, completed by Stantec in 2014, pavement structure was underlain by organic material ranging from 3.7 to 7.0 m. The site is located directly adjacent to the Pottageville Swamp Conservation Area wherein organic soil materials such as peat can be found at the surface (Figure 3-19). Inorganic soil was also observed, consisting of soft to firm clayey silt to silty clay and compact silt and sand. The groundwater level ranged from 1.5 m to 2.3 m below the surface of the existing pavement.

Figure 3-19: Highway 9 Site Location with the Local Landscape (Google Maps, 2018)

Settlement was observed on a portion of Highway 9 in 2014. Asphalt padding and other temporary repairs were considered as possible solutions to this issue, but it would only add additional weight to the current pavement structure, thus leading to potential further settlement. The potential for future repairs was a deterrent. LCC was chosen as an economical and sustainable remediation treatment to address the continued settlement, reduce safety concerns and minimize future maintenance costs. The use of LCC reduced the need of deep excavation, thus, reducing a considerable amount of excess material requiring disposal, construction time, amount of backfill material, and reducing the impact on the environment (Maher and Hagan, 2016).

The section was reconstructed in 2014. The settlement problem was observed only at the eastbound lanes, so traffic was temporarily moved to the westbound lanes. The settlement remediation treatment included excavation of a length of 100 m to a depth of 1.5 m to provide the pavement structure of:

- Asphalt concrete layer – 200 mm
- Granular "O" base layer – 200 mm
- Lightweight Cellular Concrete at the density of 475 kg/m^3 – 1100 mm
- Existing subbase

The permeability of the subgrade fill material was relatively low, so no polyethylene sheet was used to mitigate the loss of LCC material. A biaxial geogrid with a minimum tensile strength of 0.8 kN/m was installed in a LCC layer at a depth of 0.3 m below the top of the LCC.

The placement of the LCC was completed in three days. In total, 905 m^3 of LCC material was placed. Figure 3-20 demonstrates the construction process of installing the LCC layer. During the placement of cellular concrete, Quality Control (QC) testing including casting unconfined compressive strength cylinders, wet cast density, and air temperature. A list of the QC specifications is presented in Table 3-2.

Figure 3-20: Highway 9 Construction Process (CEMATRIX)

In order to mitigate the presence of water below the LCC layer, a drainage system was developed, including 1% slope of the bottom of LCC layer to the existing subgrade, a transversely installed subdrain at the end of LCC, and a longitudinally installed subdrain on the highway centerline. All these measures were done to capture water that could pond below the LCC. In addition, transition sections were arranged from both ends of the LCC section. Those transitions were critical in mitigating differential performance of LCC and adjacent sections.

Table 3-2: Project Specifications and QC Results (Maher and Hagan, 2016)

Item	Project Specification Requirements	QC Results	Average of QC Results
Minimum Unconfined Compressive Strength	1.0 MPa @ 28 days	0.9 to 1.7 MPa	1.3 MPa
Wet Cast Density	523 to 578 kg/m^3	525 to 580 kg/m^3	550 kg/m^3
Air Temperature	Protection required for sub-zero temperatures	10 to 17^0 C	14^0 C
Cellular Concrete Temperature	-	22 to 26^0 C	24^0 C
Max. Lift Thickness	500 to 600 mm	300 to 500 mm	N/A

Field visual inspection was completed in 2015, one year after construction. It was observed that the pavement was performing well. Figures 3-21 and 3-22 show that no severe distresses were found on the pavement surface. One negligible imperfection was noted in the transition area.

Another field visual inspection was completed in 2017, three years after construction. The field inspection stated that the pavement remained in good condition after three years of service. No severe cracks or rutting were observed during the inspection.

Figure 3-21: Condition of Highway 9, Three Years after Construction

Figure 3-22: Condition of Highway 9, Three Years after Construction

3.2.5 View and Vancouver Streets, City of Victoria, British Columbia, Canada

The City of Victoria was experiencing several settlements in the area around the intersection of Vancouver Street and View Street (Figure 3-23). The intersection had been reconstructed several times previously, but the major settlement issue continued to occur. Settlement was a major issue in this area because of the excessive decay and consolidation of the underlying peat. The option of removing and replacing the weak soils was proposed, but because it was an expensive and impractical procedure, finding a different solution was a priority. Moreover, since this intersection is located in the downtown area, the time of the closures played a big role in selecting a construction approach.

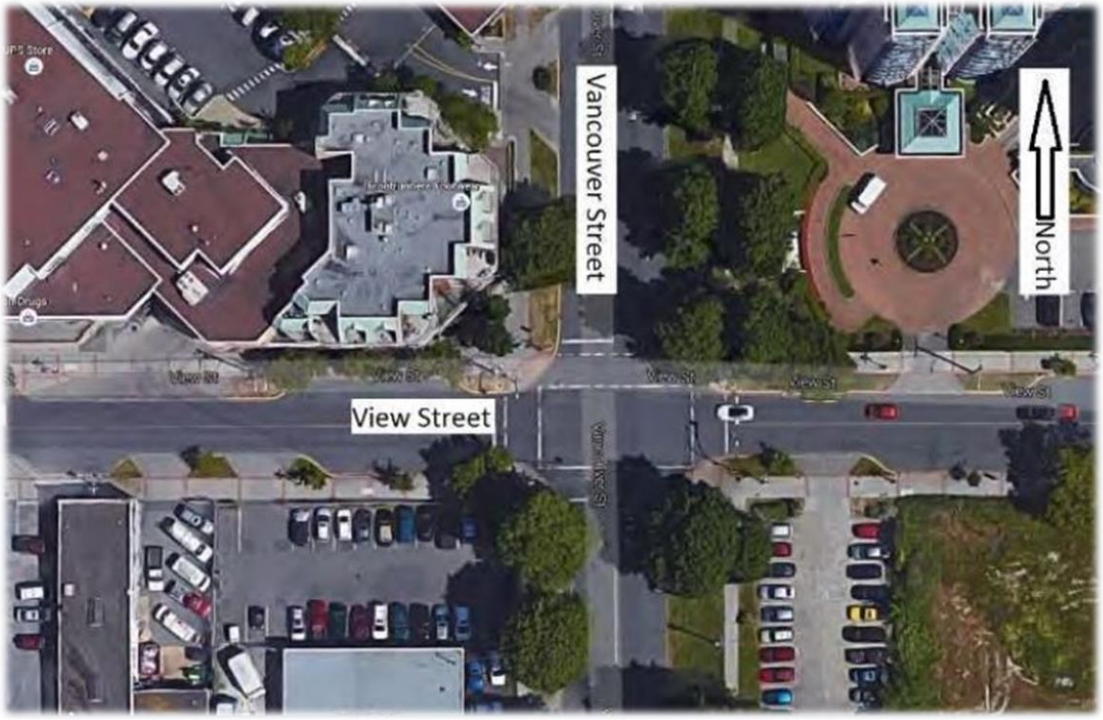

Figure 3-23: Site location. (Google maps, 2018)

Dolton et al. (2016) reported that due to excessive total differential settlement in the area, the roadways and sidewalk experienced surface distresses and damage had occurred to underlying utilities. These roadways were originally built over a peat layer that extends up to 5.3 m below the existing ground surface. Below the peat is a thick layer of soft silty clay overlying bedrock at a depth of 30 – 40 m. Use of Lightweight Cellular Concrete was chosen for this project with the following pavement structure design:

- Asphalt concrete – 75 mm
- Crush Granular base course - 150 mm of 20 mm

- LCC with wet density of 475kg/m^3 – 500 mm
- Existing subgrade

The construction at View Street and Vancouver Street in the City of Victoria, British Columbia was completed from September 2007 to April 2008 in several stages. The LCC was produced on site, and as it is shown in Figure 3-24, using the "wet" process of production (Dolton et al., 2016). LCC with wet density of 475 kg/m^3 was used as subbase in this project. Quality Assurance/Quality Control (QA/QC) testing was carried out during construction and found that cast density ranged between 435 kg/m^3 to 486 kg/m^3 with an average of 462 kg/m^3. Cylinders were also cast according to ASTM C495 for Compressive strength of LCC and results revealed an average of 1.0 MPa (range 0.8 to 1.1 MPa) at 28 days.

Figure 3-24: View Street and Vancouver Street Construction Process. Wet Mix Equipment (CEMATRIX)

Total length of the sections that were reconstructed was 430 m on View Street and 137 m on Vancouver Street with a total of 2,246 m^3 of LCC. It was placed over fourteen pour days of construction. Gravel backfill compacted with no vibration was placed on the cellular concrete before traffic was allowed on the roadway.

Golder Associates Ltd. carried out Benkelman Beam and Falling Weight Deflectometer (FWD) testing at about 20 m intervals in February 2008. The intention of the test was to carry out the test within the outer wheel paths, however, due to different obstacles, some inner wheel paths were tested as well. The weather conditions during the testing were cloudy, with an air temperature of 13^0 C and pavement temperature of 10^0 C.

The Benkelman Beam test is a method for measuring pavement deflections under static wheel loads. As presented in Figure 3-25, a 3.65 m beam is placed between the dual tires of a truck (80 kN axle load) and height measurement gauge on the end of the beam measure the vertical

rebound of the pavement after the truck is driven away (TAC, 2016). The testing was following the ASTM D 4695 "Standard Guide for General Pavement Deflection Measurements" procedure. The Benkelman Beam deflection data analysis was carried out in accordance with the Asphalt Institute MS-17 method: "Asphalt Overlays for Highway and Street Rehabilitation, Manual Series № 17". No seasonal correction factor was applied for Maximum Pavement Spring Rebound (MPSR) due to winter conditions. The average rebound was 0.63 mm on View Street and 0.65 mm on Vancouver Street (Table 3-3).

Table 3-3: Benkelman Beam Results (Golder Associates Ltd. Report, 2008)

Section	Average Rebound Reading (mm)	Temperature Corrected Rebound (mm)	Standard Deviation	Mean plus 2 STDV	MRSR (mm)
View St. New Pavement	0.63	0.73	0.15	1.03	1.03
Vancouver St. New Pavement	0.65	0.75	0.23	1.21	1.21
View St. Old Pavement	0.53	0.57	0.41	1.40	1.40

Figure 3-25: Benkelman Beam Deflection Testing

Falling Weight Deflectometer (FWD) testing was also conducted. This involves evaluating the dynamic response to the fall of the weight from a recorded height. Seven sensors were installed and spaced out at known distances from the load plate to measure deflection. FWD testing was following ASTM D 4694 "Standard Test Method for Deflections with a Falling-Weight-Type Impulse Load Device". Three load levels were used to determine the deflection response (40, 50, and 75 kN approximately) at each test point.

The measured FWD dynamic deflections were normalized to represent the equivalent deflection for a standard wheel load of 40 kN at an asphalt pavement temperature of 21^0 C. The pavement surface modulus, which indicates the overall strength of the pavement, was also determined. A summary of the FWD testing data is shown in Table 3-4**.** Spring correction factor was not applied. Results reflected consistent static deflection for the LCC sections, and that the deflection of the non-LCC section was 111% times higher than that of the LCC section. The elastic moduli of the LCC was also reported to be 445 MPa (Standard deviation 146 MPa) and 341 MPa (Standard deviation 99 MPa) which are higher than the typical values for gravel (University of Waterloo, 2011). The elastic moduli of various layers were estimated using ELMOD software (Dynatest 2006). The mean elastic modulus derived from LCC layer was inferred to be 341 MPa on View Street and 445 MPa on Vancouver Street.

Table 3-4: FWD Test Data

Street Name	Normalized Deflection (mm)				Pavement Surface Modulus (MPa)	
	Mean	Standard Deviation	Mean+ 2 STDV	Static Deflection	Mean	Standard Deviation
View St. New Pavement	0.49	0.08	0.64	1.0	361	60
Vancouver St. New	0.43	0.05	0.55	0.85	402	53
View St. Old Pavement	0.51	0.41	1.36	2.11	488	238

3.3 Summary of Case Studies

Table 3-5: Summary of the Available Cases of Using LCC as a Subbase Material in Pavement Construction in Canada

	Dixie Road. Region of Peel, Ontario	Highway 9, Holland Marsh, Ontario	View and Vancouver Streets, City of Victoria, British Columbia	Brentwood Light Rail Transit (LRT) Bus-Lane. Calgary, Alberta	Winston Churchill Boulevard, Brampton. Ontario
Location	Ontario 43°80'49.24" N 79°84'98.97" W	Ontario 44°02'52.65"N 79°61'25.19"W	British Columbia 48°42'45.48"N 123°35'67.65" W	Alberta 51°08'51.72"N 114°12'95.76" W	Ontario 43°69'87.0"N 79°92'11.0"W
Cause of Reconstruction	Settlement. Length-120m Peat/marl deposits were located from the depth of 2.1 m to 5.4 m below the existing pavement surface	Settlement. Length-100m Underlain with organic materials (peat) and inorganic (soft to firm clayey silt to silty clay or compact silt and sand)	Settlement. Length-430m on View Street and 137m on Vancouver Street. Excessive decay and consolidation of the underlying peat	Length-60m. Severe frost heave and subsequent spring thaw weakening of the frost susceptible soils.	Settlement. Length-300m. Underlain with peat.
Date of Constructio	August-November 2009	October 2014	November-February 2007	Summer (July-August) 2000	Summer 2016
Road Type	Rural highway	Highway	Urban	Urban	Rural
Structure	AC-140mm; Granular 'A'-150mm; LCC–650mm	AC-200mm; Granular "O" base layer-200mm; LCC-1100mm; Biaxial geogrid (300m from the top of LCC layer)	AC-75mm; Crushed Granular base course-150mm; LCC-500mm; (Tensar BX1100 geogrid was placed between the LCC layers)	AC-125mm; Granular base course-150mm; LCC-200mm; drainage rock-50mm; Geotextile fabric (at the bottom of LCC layer)	AC-120mm; Granular base course-240mm; LCC-550mm; geogrid reinforce fiber glass

Material Composition	CEMATRIX CMEF-475. "Dry" mix	CEMATRIX-475. "Wet" mix	CEMATRIX-475. "Wet" mix	CEMATRIX CMRI-475.	CEMATRIX-475. "Dry" mix
Performance Evaluation	Visual inspection, FWD, Benkelman Beam test	Visual inspection	FWD, Benkelman Beam test	Visual inspection, Benkelman Beam test	Visual inspection
Construction Challenges	Water, stability issues, transition areas	Transition areas, drainage, stability issues	Underlying utilities, Stability issues	Heavy traffic, stability issues	Crossfall, wet soils, stability issues

3.4 Discussions and Recommendations

Summarizing the available case studies of using LCC as a subbase in pavement construction, it is worth saying that LCC can be successfully used in rural and in urban conditions. The ages of the sections reviewed varied from two years up to 18 years, which gives an approximate understanding of pavement performances up-to-date. The oldest of the presented section is Brentwood Light Rail Transit (LRT) Bus-Lane in Calgary (18 years) and is performing well, especially in comparison to the adjacent road sections without LCC installation. The younger cases such as Winston Churchill Boulevard (Ontario), Highway 9 (Ontario) and Dixie Road (Ontario) are also performing well, with no severe cracks. The minor cracks that were observed on Dixie Road by visual survey seven years after construction are, most likely, the result of construction defects of the upper layers (GPR and FWD results confirm this theory). The road sections in the City of Victoria, British Columbia performed well up to 2010 when the last inspection was made. Unfortunately, no further performance data for this section was found.

Three out of five considered road sections are located in Ontario, approximately in one area, with similar weather conditions, one section is in Calgary, and one section is located in British Columbia.

All projects were aiming to solve a settlement problem. It is observed that settlement usually occurs on localized parts of the road and not on the whole length of the road. In four projects, the length of the reconstructions was less than 150 meters and only in one project was a longer section (the City of Victoria) needed. Moreover, this section consisted of two intersecting roads, which formed a bigger area of settlement.

The common time for construction was summer-fall time as the soil is more stable and no freeze-thaw cycles are occurring and the subgrade is thawed. Most of the projects were done in July-November and none in the spring.

In terms of the structure of the sections, they all follow the same pattern: LCC layer at the bottom (usually with the geogrid or geotextile reinforcement), followed by Granular base material and asphalt concrete layer at the top. The thicknesses of the layers are different, depending on the purpose of the road and underlying soil.

FWD and Benkelman Beam tests are the most commonly used methods for evaluating the performance of the LCC sections to date.

Some projects were using "dry" mix process and some "wet". It is common to use "dry" mix process of producing the material for the projects, where relatively high volumes of LCC were needed. However, in the City of Victoria, the installation process happened in three stages and in different months because of the specific road closures and downtown location of the road. In that project, "wet" mix process was used.

In order to use LCC in a pavement structure as a subbase, certain activities have to be taken into consideration and implemented into the construction process. A number of general observations that are applicable to most LCC projects have been made from studying the road sections across Canada. These observations are presented in the following paragraphs.

Soils

Generally, the main issue that using LCC is intended to addresses is a process of settlement of road sections. In most of the case studies, settlement is happening because of weak subgrade soils. It can be either organic material (peat) or inorganic soils (soft to firm clayey silt to silty clay or compacted silt and sand). Placing a thick layer of unbound granular material on top of those subgrade types, to solve the settlement issue, may lead to more settlements in the future due to the excessive weight of the whole structure. In addition to that, a lot of excavation is often needed to remove the weak soil before placing the unbound Granular material.

Water

Placement of the LCC during light rain is possible but should be avoided in heavy rain. Water is a significant factor, influencing the construction of pavements using LCC. Groundwater seepage control of the excavations, where LCC will be placed, is required. This needs to be done to prevent floating of the material, as the target density of LCC in the case studies was 475 kg/m^3, which is less than water density (1000 kg/m^3). Ignoring water presence in the excavations may lead to buoyancy forces affecting the pouring and restarting the production and placement from the very beginning may be required.

Drainage

It is very important to prevent moisture from weakening the pavement structure once it is in-service. Usually, pavements require a slope of 2% in order to let the stormwater from the surface of the pavement, and subsurface water to drain by the gravity force. For achieving the 2% slope, LCC must be placed in steps, using formwork.

Transitions

Constructing the quality and proper transition areas between pavement sections with LCC and conventional granular pavement is crucial. Those two different pavement structures have different thermal properties and different densities. Because of that, different performance of the pavement structures can occur in those areas during the freeze-thaw conditions. As frost is unlikely to penetrate through the LCC pavement due to its high porosity, reverse heaving of the transition occurs (Maher and Hagan, 2016). In order to mitigate this effect, granular transition tapers can be made in the transition areas. The commonly used is a 10/1 ratio of horizontal to vertical respectively.

Equipment

All the material brought to site must be transported in pre-cleaned equipment and machinery. The transporting equipment must be cleaned, rinsed and completely emptied of the concrete, aggregates, and any other materials that were previously transported (Maher and Hagan, 2016). This was a general consideration in the case studies that were using "dry" mix process; however, for the View Street and Victoria Street intersection, that used "wet" mix process, it was a significant consideration.

This study provides an overview of the current pavement condition of the five sections that were constructed using lightweight cellular concrete as subbase layer material. Results have shown that all five sections were in good pavement condition. However, in-depth pavement data collection has to be done in order to provide a comprehensive review of the performance of the sections with lightweight cellular concrete as subbase layer. Therefore, further investigation is recommended. This could be achieved by using pavement instrumentation such as asphalt gauges, earth pressure cells, and environmental equipment in the new pavement structures.

CHAPTER 4

4 PAVEMENT DESIGN AND ANALYSIS

This Chapter explains the procedure on how pavement design for LCC can be conducted. The predicted performance of the LCC road sections will be determined by failure criteria analysis. Comparison of LCC section to typical Granular material will also be conducted.

4.1 Introduction into Pavement Design

Structural design of pavements is a complex process. Several factors have to be considered when designing a road. These factors are traffic (axle or gear loads, repetitions), environment, available materials, desirable performance of the pavement, project cost, sustainability, and construction resources (TAC, 2013).

Traffic volume is usually described by Annual Average Daily Traffic (AADT), which shows the range of vehicles of various sizes, weights, and axle configurations. The 80 kN standard single axle is used for quantifying the traffic in pavement design. It allows transition of the cumulative damage from the range of vehicles into a number of Equivalent Single Axle Loads (ESALs) (ARA, 2015).

Climate is another factor that should be considered in pavement design. According to Applied Research Associates (2015), information about pavement surface temperatures expected for the south and east region of Ontario are summarized in Appendix II**.**

The above-stated factors and some others, that have significant influence on pavement performance, are implemented in several mechanistic pavement models. One of the commonly used ones is Mechanistic-Empirical Pavement Design Guide (MEPDG), which was developed to predict the deterioration of pavements and their associated expected service lives. The focus of this chapter is studying the pavement structure, although some approximate service life of the pavement without any maintenance was also estimated. The WESLEA software was used in this research - a linear elastic multi-layer program that enables analysis of a pavement structure, including the effects of complex load systems.

4.2 Pavement Design with Lightweight Cellular Concrete (LCC)

The structure of the typical pavement, with respect to the usage of LCC as a subbase, usually consists of LCC layer placed on the subgrade, followed by unbound Granular base material and the asphalt concrete layer as a top surface. Typical pavement structure with LCC is presented in Figure 4-1. Even though the LCC is different from traditional granular material and should be treated as a cement stabilized material, there are no calibration factors and performance models designed for the lightweight cellular concrete. In the MEPDG manual, it is noted that if

the cement stabilized base layer is beneath an unbound Granular base and hot-mix asphalt layer, the pavement design should treat it as an unbound layer with a constant layer modulus.

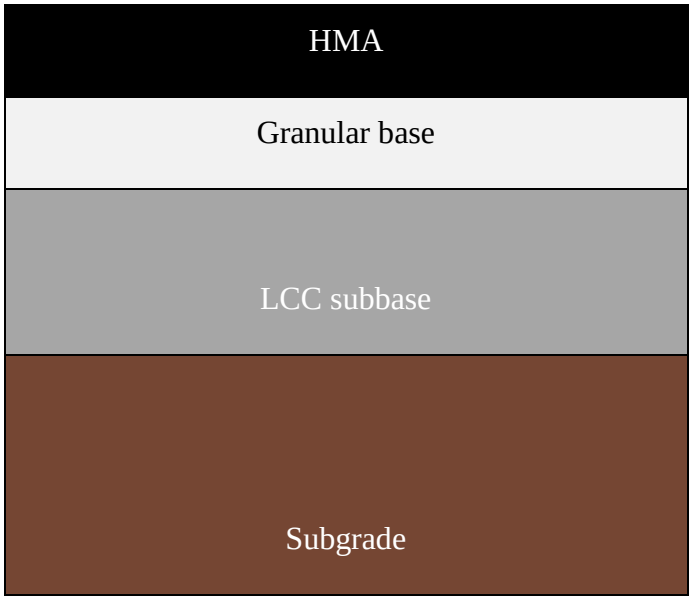

Figure 4-1: Pavement Structure with LCC

4.3 Analysis Method

Three roads in Ontario with installed LCC were chosen to be studied: Dixie Road, Highway 9 and Winston Churchill Boulevard. This Chapter aims to predict performance of the installed LCC sections in terms of fatigue cracking and rutting issues as well as to determine the bearing capacity of the road sections. These parameters were discussed as the failure criteria. Furthermore, the comparison between LCC and Granular B subbase materials that were installed on the same road sections was completed and discussed. The predicted service life of the pavements without any maintenance was determined.

The method for the failure criteria analysis consisted of the following approaches:

- Measuring the response of the pavement to different loadings. At this approach, the ability of the pavement to withstand various loads was studied by controlling stress values at the bottom and top of the subbase layer.
- Determining the allowable number of load repetitions on the pavement. The approach obtains the number of maximum load repetitions that can be withstand by the pavement.
- Identifying the maximum ESALs that road section can bear. Damages due to cumulative Equivalent Single Axle Loads were determined and presented in the graphs as potential fatigue cracking and rutting issues.

4.4 Failure Criteria Analysis

In order to understand the expected vertical stress and tensile stress that will occur in the pavement structure the failure criteria analysis was conducted using the WESLEA software. The pavement structure and material properties were taken from the existing projects in Canada. Some unknown values were assumed in this analysis based on engineering experience and recommended values (TAC, 2014). Modulus of elasticity for LCC was taken as 850 MPa as a result of the tests that were conducted by the author's colleagues in CPATT laboratory (for the LCC density of 475 kg/m^3).

Two types of pavement structure using a different material for subbase layer were analyzed and compared, which are the Lightweight Cellular Concrete and the unbound Granular B subbase material. The pavement structure and material properties are provided in Table 4-1.

ESALs for Dixie Road were taken from the report completed by Griffiths and Popik (2013). The AADT information for Highway 9 was obtained from MTO (provincial highways traffic volumes 2016 report). The ESALs for Dixie Road and for Winston Churchill Boulevard were predicted to be 500,000 and 160,000 respectively (Table 4-2).

Table 4-1: WESLEA Settings for Dixie Road, Highway 9 and Winston Churchill Boulevard (Material Properties of the Pavement)

		Surfac	Base	Subbase		Subgrad
		HMA	Granular	Granular B	LC	Soil
Dixie Road	E (MPa)	3445	250	200	850	30
	Poisson's Ratio	0.35	0.4	0.35	0.2	0.45
	Thickness (mm)	140	150	650	650	-
Highway 9	E (MPa)	3445	250	200	850	30
	Poisson's Ratio	0.35	0.4	0.35	0.2	0.45
	Thickness (mm)	200	200	1100	1100	-
Winston Churchill Blvd	E (MPa)	3445	250	200	850	30
	Poisson's Ratio	0.35	0.4	0.35	0.2	0.45
	Thickness (mm)	120	240	550	550	-

Table 4-2: ESALs for Three Road Sections in Ontario

	Dixie Road	Highway 9	Winston Churchill Blvd
ESALs	500,000	1,500,000	160,000

LCC is a potential substitution of the granular material for the subbase in some projects. This chapter aimed to compare the predicted performance of the pavements with LCC with the same road but with granular material; thus the same steps for determining the stress values were taken for both pavements – LCC and granular subbase pavements.

4.4.1 First Approach

With the use of WESLEA software, the vertical stress and tensile stress happened on the top of the subbase layer and bottom of the subbase layer respectively at different loads is shown in Figure 4-2. To develop the graphs, the load range was varied from 20 kN to 120 kN of magnitude. The standard axle load number is usually considered to be 80 kN. Figure 4-2 presents the expected vertical stress that will be applied to the subbase layer.

The vertical stress applied to the LCC layer is higher than the one to the Granular B layer for every loading set for all three roads. However, the typical compressive strength of the LCC at low density ranges between 0.5 MPa to 1.0 MPa. Thus, the LCC layer is considered strong enough to support the pavement in the range of 20 kN to 120 kN of axle loads. The output of the WESLEA software is shown in Tables 4-3; 4-4; 4-5.

Table 4-3: Vertical and Tensile Stresses. Dixie Road

Dixie Road				
Load, kg	Vertical Stress at the Top of Granular B	Tensile Stress at the Bottom of Granular B	Vertical Stress at the Top of LCC layer	Tensile Stress at the Bottom
2000	55.53	-25.07	83.21	-45.68
4000	105.18	-49.63	156.01	-90.35
6000	150.34	-73.68	220.81	-134.04
8000	191.9	-97.24	279.2	-176.79
10,000	230.47	-120.32	332.28	-218.62
12,000	266.47	-142.93	380.84	-259.57

Table 4-4: Vertical and Tensile Stresses. Highway 9

Highway 9				
Load, kg	Vertical Stress at the Top of Granular layer	Tensile Stress at the Bottom of Granular Layer	Vertical Stress at the Top of LCC layer	Tensile Stress at the Bottom of LCC Layer
2000	34.27	-10.14	52.84	-18.68
4000	66.56	-20.19	102.11	-37.19
6000	97.12	-30.14	148.27	-55.51
8000	126.14	-40.01	191.67	-73.66
10,000	153.79	-49.78	232.57	-91.63
12,000	180.19	-59.47	272.2	-109.43

Table 4-5: Vertical and Tensile Stresses. Winston Churchill Blvd

Winston Churchill Boulevard				
Load, kg	Vertical Stress at the Top of Granular layer	Tensile Stress at the Bottom of Granular Layer	Vertical Stress at the Top of LCC layer	Tensile Stress at the Bottom of LCC Layer
2000	52.64	-0.92	74.72	-1.85
4000	101.26	-1.76	142.88	-3.56
6000	146.46	-2.51	205.46	-5.11
8000	188.7	-3.17	263.21	-6.53
10,000	228.31	-3.76	316.72	-7.82
12,000	265.58	-4.27	366.43	-8.97

The results of the tensile stress occurring at the bottom of the subbase layer are demonstrated in Figure 4-2. It is clear that the tensile stress happening at the LCC layer is higher than the tensile stress occurring at the Granular B layer. However, according to Narayanan and Ramamurthy (2000), the flexural strength of lightweight cellular concrete ranges from 15% to 35% of its compressive strength, which is between 0.075 to 0.35 MPa for the typical low-density lightweight cellular concrete. Predicted maximum value obtained from the WESLEA

software for tensile stress at the bottom of the LCC subbase layer (at 120 kN load magnitude) throughout all road sections was 0.26 MPa. The right part of Figure 4-2 displays that both of the subbase layers for all three roads are capable of resisting the tensile stress and protect the layer from damage.

Maximum vertical stresses that potentially could happen under 120 kN load magnitude at the top of LCC layer were 0.38 MPa, 0.27 MPa and 0.36 MPa for Dixie Road, Highway 9 and Winston Churchill Boulevard respectively. Those values are lower than typical compressive strength values for the Lightweight Cellular Concrete (0.5 to 1.5 MPa). Thus, LCC layer can potentially hold the vertical stress without being damaged (Figure 4-2).

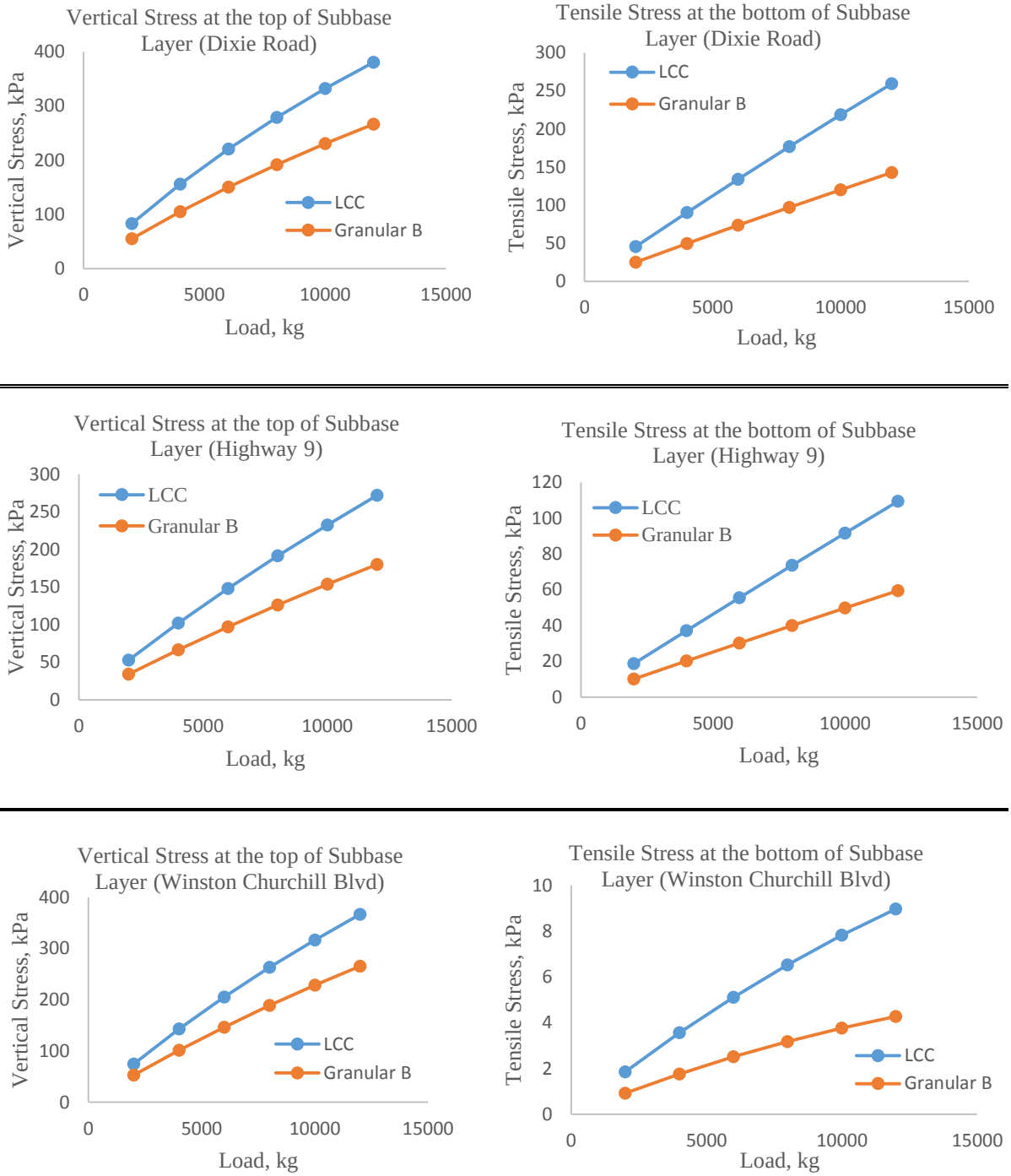

Figure 4-2: Vertical and Tensile Stresses. Comparison for Dixie Road, Highway 9 and Winston Churchill Blvd (WESLEA software, 2018)

4.4.2 **Second Approach**

The vertical stress value at the bottom of AC layer and tensile strength at the bottom of LCC layer were taken as the representatives of the fatigue and rutting measures respectively. By using the WESLEA software, damage analysis for fatigue cracking and permanent deformation was obtained. The equations that were used in the calculation of fatigue cracking and rutting in WESLEA software are presented below:

$$N_{fc} = 2.83 \times 10^{-6} \left(\frac{10^6}{\varepsilon_t}\right)^{3.148} \quad (1)$$

Where:

Nfc = Allowable number of load repetition before fatigue cracking

ε t = Tensile strain at the bottom of surface layer

$$N_{fr} = 1.0 \times 10^{16} \left(\frac{1}{\varepsilon_v}\right)^{3.87} \quad (2)$$

Where:

N_{fr}= Allowable number of load repetition before rutting

ε v = Compressive strain at the top of subgrade layer

The output of the WESLEA software of the predicted damage to the pavements is presented in Tables 4-6; 4-7; 4-8.

Table 4-6: Allowable Number of Load Repetition. Fatigue Cracking and Rutting for Dixie Road

Dixie Road				
Load, kg	Fatigue. Pavement with Granular B	Rutting. Pavement with Granular B	Fatigue.Pavement with LCC	Rutting.Pavement with LCC
2000	2,417,552	12,264,561	4,602,352	154,158,424
4000	451,514	870,860	1,005,395	10,962,335
6000	183,018	188,197	443,908	2,372,274
8000	107,632	64,135	287,635	809,479
10,000	76,547	28,049	227,081	354,437
12,000	60,720	14,631	200,912	181,681

It should be noted that the LCC layer could potentially carry more traffic loading than Granular B layer before fatigue cracking happens. This conclusion can be made due to the fact that the Total Allowable Number of Load Repetition (in terms of fatigue cracking) of LCC layer is 1.4 to 3.3 times higher than the Granular B layer depending on the project. Giving the example of the typical axle load of 80 kN for Dixie Road, the Total Allowable Number of Load Repetition with LCC is 287,635 whereas it is 107,632 with Granular B. The ratio comes to 2.67, meaning that pavement with LCC is superior in terms of resistance to fatigue cracking.

Table 4-7: Allowable Number of Load Repetition. Fatigue Cracking and Rutting for Highway 9

Highway 9				
Load, kg	Fatigue. Pavement with Granular B	Rutting. Pavement with Granular B	Fatigue.Pavement with LCC	Rutting.Pavement with LCC
2000	8,801,919	348,501,635	15,268,311	5,148,891,932
4000	1,335,740	24,233,438	2,433,609	358,295,756
6000	500,772	5,129,902	962,659	75,899,446
8000	269,727	1,712,909	548,875	25,360,318
10,000	175,802	734,178	379,512	10,876,822
12,000	128,467	368,512	294,602	5,462,865

Table 4-8: Allowable Number of Load Repetition. Fatigue Cracking and Rutting for Winston Churchill Boulevard

Winston Churchill Boulevard				
Load, kg	Fatigue. Pavement with Granular B	Rutting. Pavement with Granular B	Fatigue. Pavement with LCC	Rutting. Pavement with LCC
2000	1,605,741	8,847,648	2,279,127	90,925,930
4000	343,393	630,873	538,184	6,482,740
6000	145,964	136,897	241,716	1,406,532
8000	90,887	46,842	160,580	481,185
10,000	68,516	20,567	130,016	211,232
12,000	57,474	10,572	117,682	108,552

The results for predicted rutting performance show even stronger differentiation between values. The performance of the LCC based pavements in terms of rutting is from 10.2 to 14.8 times better than with Granular B. For Highway 9, under the typical axle load of 80 kN, the Total Allowable Number of Load Repetition with LCC and Granular B (in terms of rutting) is 25,360,318 and 1,712,909 respectively. Thus giving the ratio of 14.8. This is due to the fact that LCC material is stiffer itself and because rutting is a result of tensile stress at the bottom of the subbase layer, LCC-based pavements show lower rutting issues.

The results of the Allowable Number of Load Repetition under the various loadings are shown in Figure 4-3. It is clear that the pavement with LCC subbase is more durable than the pavement with Granular B layer at the same thickness since the allowable numbers of load repetitions for fatigue cracking and permanent deformation are higher.

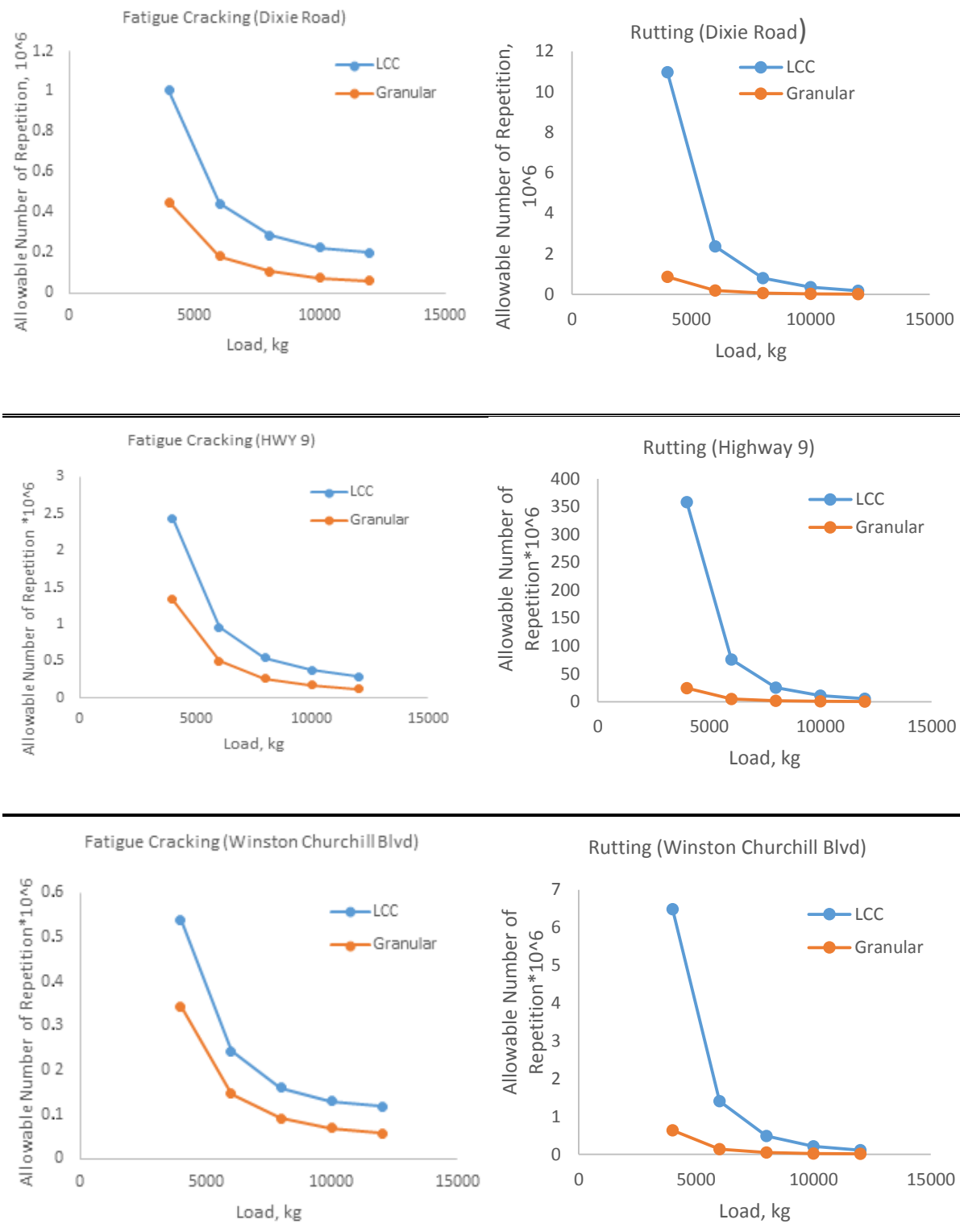

Figure 4-3: Allowable Number of Load Repetition. Fatigue Cracking and Rutting for Dixie Road, Highway 9 and Winston Churchill Blvd (WESLEA software, 2018)

4.4.3 **Third Approach**

In order to understand the approximate service life of the pavement without any maintenance, Allowable Number of Load Repetitions vs ESALs graphs were plotted on Figure 4-4. The maximum Allowable Number of Load Repetitions was calculated by WESLEA software and it was 107,632 for fatigue cracking and 64,135 for rutting (Dixie Road; Granular-based section). In comparison, for LCC-based section for the same road, those values were 287,635 and 809,479 for fatigue cracking and rutting respectively. Values for other sections are presented in Tables 4-11; 4-12; 4-13; 4-14.

The ratio between the range of ESALs and Allowable Number of Load Repetitions was calculated in order to predict the capacity of the particular section. If the damage ratio exceeds one, it indicates that a failure could happen on the pavement as traffic loading surpass the pavement's bearing capacity. Damage ratio under various ESALs for each road section were calculated to determine bearing capacity of the pavements under different traffic loading. Satisfactory result was considered when both rutting and fatigue cracking damage ratio were below one. For Dixie Road, Granular-based pavement, this number was 50,000 ESALs, whereas for the LCC-based it was 250,000 ESALs (Table 4-9; 4-10). The same trend was observed on two other roads – Highway 9 and Winston Churchill Boulevard. For Highway 9 (Tables 4-11; 4-12), both fatigue and rutting damage ratio were lower than one under the 100,000 ESALs (Granular layer) and 500,000 ESALs (LCC layer). For Winston Churchill Boulevard – 40,000 and 160,000 ESALs respectively (Tables 4-13; 4-14).

All three road sections installed with LCC as a subbase could potentially withstand higher ESALs than pavements with Granular material. This can lead to the conclusion that LCC-based pavements could be more durable in terms of fatigue cracking and rutting resistance.

The output from the WESLEA software of the predicted damage of the pavements is presented in Tables 4-9; 4-10; 4-11; 4-12; 4-13; 4-14.

Table 4-9: Predicted Damage (Fatigue Cracking and Rutting) of Pavement with Granular B Subbase. Dixie Road (WESLEA, 2018)

Granular B					
		Fatigue cracking. With Granular B		Rutting. With Granular B	
Load,kg	ESALs	Allowable	Damage	Allowable	Damage
80	500,000	107,632	4.65	64,135	7.80
80	450,000	107,632	4.18	64,135	7.02
80	400,000	107,632	3.72	64,135	6.24
80	350,000	107,632	3.25	64,135	5.46
80	300,000	107,632	2.79	64,135	4.68
80	250,000	107,632	2.32	64,135	3.90
80	200,000	107,632	1.86	64,135	3.12
80	150,000	107,632	1.39	64,135	2.34
80	100,000	107,632	0.93	64,135	1.56
80	50,000	107,632	0.46	64,135	0.78

Table 4-10: Predicted Damage (Fatigue Cracking and Rutting) of Pavement with LCC Subbase. Dixie Road (WESLEA, 2018)

LCC					
		Fatigue cracking. With LCC		Rutting. With LCC	
Load, kg	ESALs	Allowable	Damage	Allowable	Damage
80	500,000	287,635	1.74	809,479	0.62
80	450,000	287,635	1.56	809,479	0.56
80	400,000	287,635	1.39	809,479	0.49
80	350,000	287,635	1.22	809,479	0.43
80	300,000	287,635	1.04	809,479	0.37
80	250,000	287,635	0.87	809,479	0.31
80	200,000	287,635	0.70	809,479	0.25
80	150,000	287,635	0.52	809,479	0.19
80	100,000	287,635	0.35	809,479	0.12
80	50,000	287,635	0.17	809,479	0.06

Table 4-11: Predicted Damage (Fatigue Cracking and Rutting) of Pavement with Granular Subbase. Highway 9 (WESLEA, 2018)

Granular B					
		Fatigue cracking. With Granular B		Rutting. With Granular B	
Load, kg	ESALs	Allowable	Damage	Allowable	Damage
80	1,500,000	269,727	5.56	1,712,909	0.88
80	1,300,000	269,727	4.82	1,712,909	0.76
80	1,100,000	269,727	4.08	1,712,909	0.64
80	900,000	269,727	3.34	1,712,909	0.53
80	700,000	269,727	2.60	1,712,909	0.41
80	500,000	269,727	1.85	1,712,909	0.29
80	300,000	269,727	1.11	1,712,909	0.18
80	100,000	269,727	0.37	1,712,909	0.06

Table 4-12: Predicted Damage (Fatigue Cracking and Rutting) of Pavement with LCC Subbase. Highway 9 (WESLEA, 2018)

LCC					
		Fatigue cracking. With LCC		Rutting. With LCC	
Load, kg	ESALs	Allowable	Damage	Allowable	Damage
80	1,500,000	548,875	2.73	25,360,318	0.06
80	1,400,000	548,875	2.55	25,360,318	0.06
80	1,300,000	548,875	2.37	25,360,318	0.05
80	1,200,000	548,875	2.19	25,360,318	0.05
80	1,100,000	548,875	2.00	25,360,318	0.04
80	1,000,000	548,875	1.82	25,360,318	0.04
80	900,000	548,875	1.64	25,360,318	0.04
80	800,000	548,875	1.46	25,360,318	0.03
80	700,000	548,875	1.28	25,360,318	0.03
80	600,000	548,875	1.09	25,360,318	0.02
80	500,000	548,875	0.91	25,360,318	0.02

Table 4-13: Predicted Damage (Fatigue Cracking and Rutting) of Pavement with Granular Subbase. Winston Churchill Boulevard (WESLEA, 2018)

Granular B					
Input Parameters		Fatigue cracking. With Granular B		Rutting. With Granular B	
Load, kg	ESALs	Allowable	Damage	Allowable	Damage
80	160,000	90,887	1.76	46,842	3.42
80	145,000	90,887	1.60	46,842	3.10
80	130,000	90,887	1.43	46,842	2.78
80	115,000	90,887	1.27	46,842	2.46
80	100,000	90,887	1.10	46,842	2.13
80	85,000	90,887	0.94	46,842	1.81
80	70,000	90,887	0.77	46,842	1.49
80	55,000	90,887	0.61	46,842	1.17
80	40,000	90,887	0.44	46,842	0.85

Table 4-14: Predicted Damage (Fatigue Cracking and Rutting) of Pavement with LCC Subbase. Winston Churchill Boulevard (WESLEA, 2018)

LCC					
Input Parameters		Fatigue cracking. With LCC		Rutting. With LCC	
Load, kg	ESAL	Allowable	Damage	Allowable	Damage
80	220,000	160,580	1.37	481,185	0.6
80	200,000	160,580	1.25	481,185	0.42
80	180,000	160,580	1.12	481,185	0.37
80	160,000	160,580	1.00	481,185	0.33
80	140,000	160,580	0.87	481,185	0.29
80	120,000	160,580	0.75	481,185	0.25
80	100,000	160,580	0.62	481,185	0.21
80	80,000	160,580	0.50	481,185	0.17
80	60,000	160,580	0.37	481,185	0.12
80	40,000	160,580	0.25	481,185	0.08
80	20,000	160,580	0.12	481,185	0.04

Figure 4-4 shows the comparison between LCC and Granular materials in terms of performance. In all three roads, LCC-based pavements showed good performance in terms of fatigue cracking and rutting. In all cases, except for the fatigue cracking resistance on Dixie Road, pavements with LCC layer showed potential ability to resist the load. For Dixie Road, the ESALs of 500,000 was higher than one obtained from the WESLEA software of 250,000 ESALs, meaning that pavement cannot withstand this large number of ESALs without any maintenance. In terms of rutting, there was a significant margin in LCC-based pavements before they reached the allowable limit of load repetitions. By modeling different pavement structures (LCC and Granular B based) there is an opportunity to visually estimate the difference between the two performances. According to WESLEA output, LCC has performed better in all three projects in both fatigue cracking and rutting resistance. It should be noted that the difference in the performance of the sections was more significant in terms of rutting.

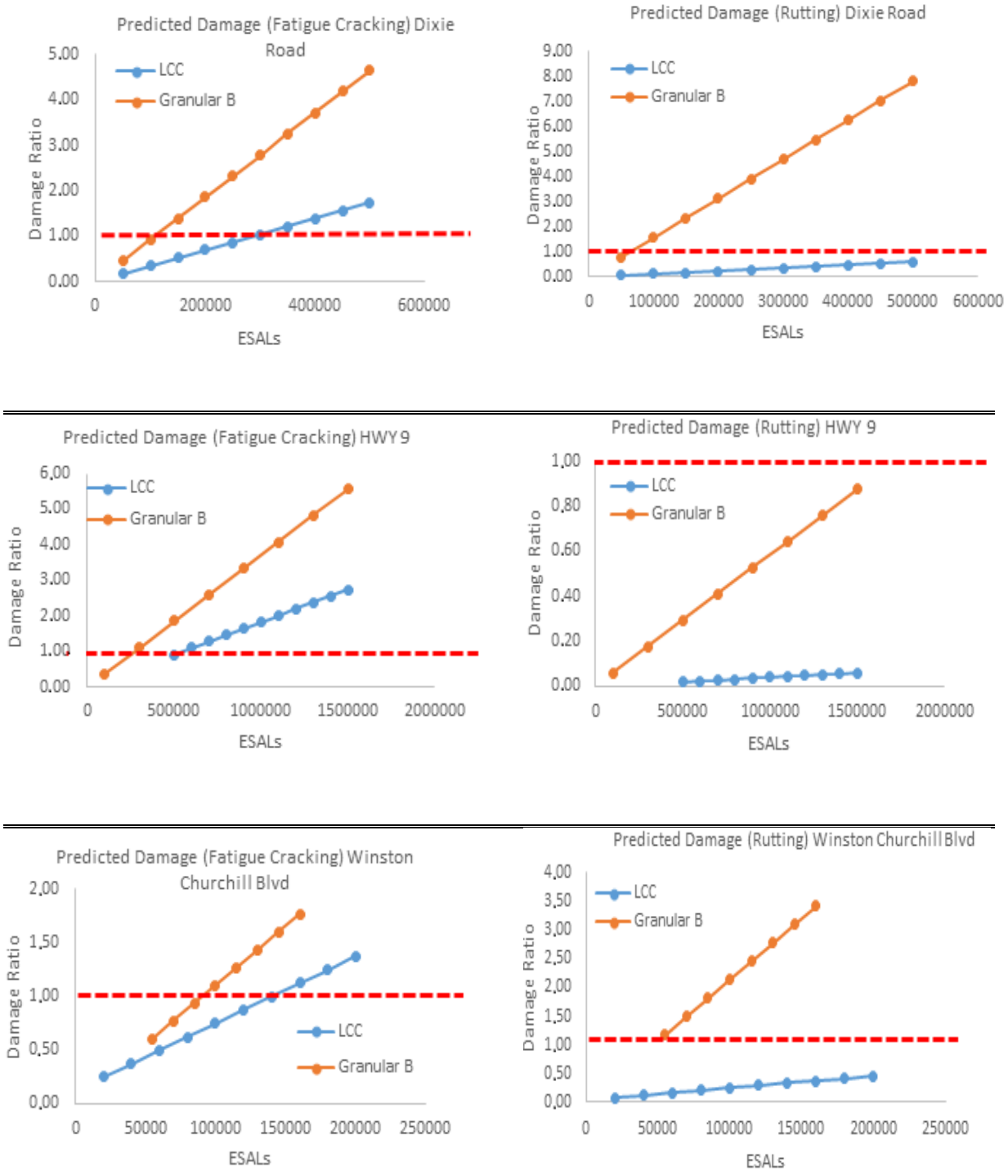

Figure 4-4: Predicted Damage. Fatigue Cracking and Rutting for Dixie Road, Highway 9 and Winston Churchill Blvd (WESLEA Software, 2018)

4.5 Summary

Three roads in Ontario were taken as examples of roads with settlement issues. All three sections were installed with the LCC layer as a subbase and prediction performance of those sections was determined by the criteria analysis.

The result of the failure criteria analysis indicated that the LCC layer is more durable compared to the conventional Granular B materials; thus, pavement thickness using LCC as a subbase material could be thinner than the conventional pavement structure, which may reduce the excavation depth during construction and save time and money. This also shows that using LCC as a subbase layer material could be effective. However, the software does not consider the environmental impact such as temperature and moisture. An in-situ field inspection is needed to evaluate the environmental effect on the pavement using LCC as a subbase layer. The results of the failure criteria analysis indicated that the usage of LCC as a subbase material is more durable than the conventional granular material with similar thickness. The findings demonstrate that LCC could be considered as a potential pavement subbase material in respect to mechanical properties. However, other durability and functional properties have to be assessed.

CHAPTER 5

5 TORONTO PROJECT

Mechanical properties of LCC samples, cast during constructing project will be studied in this Chapter. Results, obtained from the laboratory testing will be compared to the typical values for LCC in the literature.

All of the road sections described and studied in Chapters 3 and 4 were constructed prior to this research being carried out. In order to study the current state and condition of the sections installed with Lightweight Cellular Concrete (LCC) and, to predict the future performance of the pavement, laboratory tests on defining mechanical properties of LCC needed to be done. Some companies, such as CEMATRIX, have been running laboratory tests by using their own laboratories as well as using third-party companies. Typically, preparation of samples in laboratory conditions might not necessarily reflect actual site construction conditions. This could be due to a number of unforeseen circumstances that might occur during the construction process, including but not limited to weather conditions, challenges with equipment and human factor. As a result of this, it is important to assess the characteristics of the actual field-cast material. Therefore, this study obtained LCC samples from the actual site and tested them in the CPATT laboratory. Some of the most important mechanical properties such as Modulus of Elasticity, Poisson's ratio, and UCS were determined and compared to the typical values for the corresponding LCC densities.

5.1 Site Description

One of the ongoing projects Southern Ontario is a road section of Eglinton Avenue West, East of Black Creek Drive, Toronto, Ontario (Figure 5-1). The purpose of this project is to widen the road. This construction project consists of several measures including but not limited to constructing a retaining wall out of concrete and raising the surface of the road by approximately five meters. The latter was designed to be installed with lightweight material since the reduction in weight of this thick pavement layer was required.

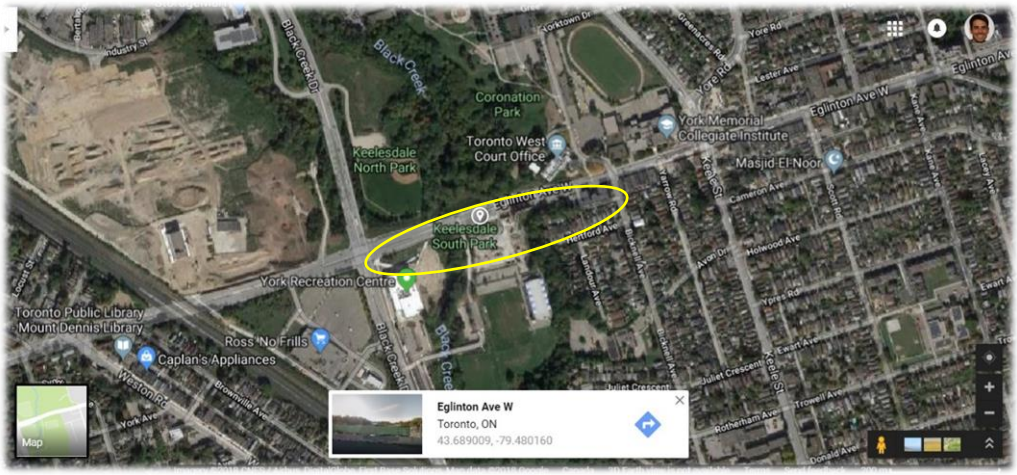

Figure 5-1: Site Location (Google Maps, 2018)

5.2 Approach

The aim of this Chapter is to determine mechanical properties of the in-situ cast samples and to compare the obtained values to the typical values in literature. In addition, the relationship between the mechanical properties of LCC will be discussed.

Access to the construction site for collecting the fresh samples was provided by the company, which was conducting the Lightweight Cellular Concrete work (CEMATRIX). A total of 2521 m^3 of LCC material was poured over a couple of weeks. As part of this project, cylindrical molds were prepared for casting the LCC samples by University of Waterloo team. Modulus of elasticity, unconfined compressive strength, and Poisson's ratio were determined by testing those samples.

5.3 Production and Placement

Lightweight Cellular Concrete with the 475 kg/m^3 plastic density was used in this project. The "dry" mix process was utilized. The composition of the mix was cement (80%), slag (20%), w/c ratio of 0.5 and a foaming agent. The cement and slag were mixed together by a contractor before deliver to the site and after that, this dry mix was sucked into CEMATRIX "dry" mix equipment where it was blended with water. Figure 5-2 represents the construction process.

Figure 5-2: Construction Process. Toronto, May 2018

The target plastic density and the slurry temperature were controlled at this stage. Quality Control (QC) is one of the steps for checking the desirable features of the mix. Marsh cone test was conducted to ensure the mix met the desired requirement. According to industrial experience, it is found that 45 to 90 seconds in Marsh cone test could provide a stable and quality cement slurry.

After mixing the slurry, the mix is pumped to the site through a hose. At the same moment, the foaming agent is added to the mix and it is blended while moving inside the hose. In order to blend the LCC mix properly, a special device is installed in the beginning of the hose, which twists the torrent.

Plastic density was checked once per every 100 m^3 during the pouring to ensure the target plastic density was reached and maintained. No consolidating and vibrating during the placement process was carried out as it may harm the bubble structure of the material.

During the placement of the LCC mix, several buckets were filled with material. Shortly after that, all the prepared molds were cast from the above-mentioned buckets prefilled with LCC (Figure 5-3). The target density for LCC material was 475 kg/m^3. According to Maher and Hagan, (2016) plastic density may vary in the range of ±10% of designed density. Thus, the range for the 475 kg/m^3 LCC mix is 427.5 to 522.5 kg/m^3. During the mixing on site, Quality Control showed that the average plastic density of the mix was 454 kg/m^3.

Figure 5-3: Samples, Collected on Site. 75*150 mm Molds for UCS test. 150*300 mm Molds for Modulus of Elasticity and Poisson's Ratio Tests

The following sections discuss the laboratory tests that were performed such as Unconfined Compressive Strength, Modulus of Elasticity and the Poisson's ratio. Samples for UCS test were collected in the amount of four samples per each test date. UCS testing was performed on 7, 14, 21 and 28th days. In addition, several samples were collected as spare samples for setting up the testing equipment. Modulus of elasticity and Poisson's Ratio test was conducted on 28th day only. Seven samples, including dummy ones, of 150 mm*300 mm were collected for testing modulus of elasticity and Poisson's ratio. The procedures followed for each test are described below.

5.4 Laboratory Tests

Laboratory tests were conducted at the University of Waterloo, at the Centre for Pavement Transportation and Technology (CPATT) laboratory from June 1, 2018 to June 22, 2018.

5.4.1 **Unconfined Compressive Strength**

This test was carried out in accordance with ASTM C495 and ASTM C796. Four cylinder specimens with dimensions 75 mm by 150 mm were tested. The samples were cast in-situ and in order to prevent them from being broken and to avoid compaction from vibration, samples were kept on site for three days. The ambient temperature on May 25th to May 27th, during the field work, is presented in Figure 5-4.

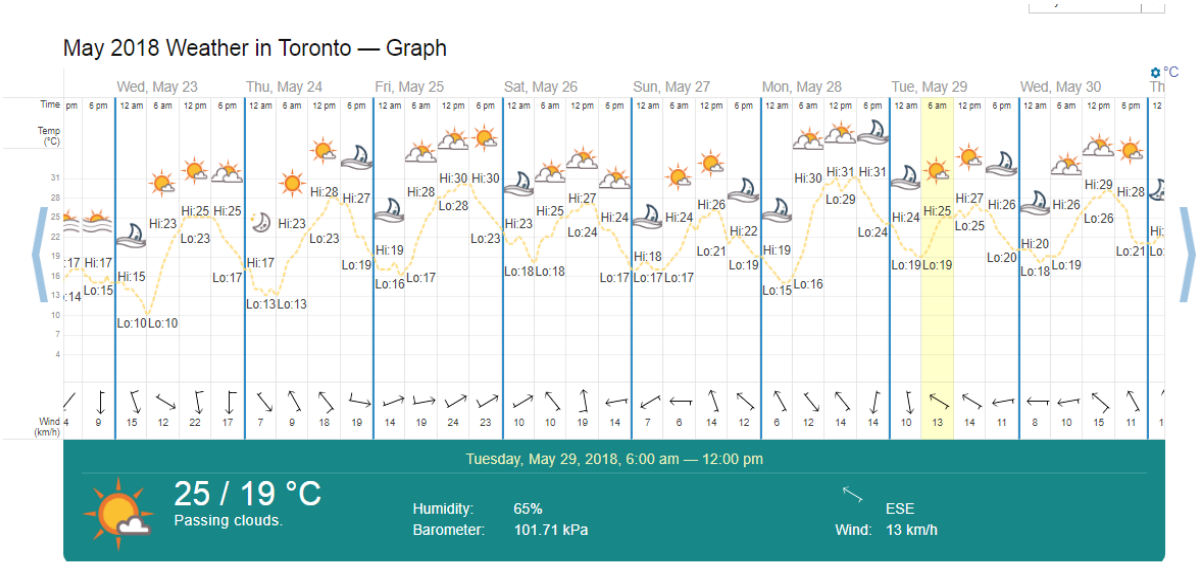

Figure 5-4: Weather Forecast during Construction and Casting the Samples (https://www.timeanddate.com/weather/canada/toronto/historic?month=5&year=2018)

Later, samples were cured at room temperature 21±6^{0}C from day four to the testing day. Before testing the samples, they were demolded, grinded at the top and the bottom in order to have horizontal flat surfaces. Measurements of the samples were taken such as height, diameter, and weight. The average measured hardened state densities for the different batches of samples were reported as 416, 408, 410, 401 kg/m^3. The actual density, which is known as a hardened state density, was observed to be lower than plastic density of material that was poured on site. The hardened state density of LCC is typically about 80 kg/m^3 less than its plastic density (Legatski, 1994). Thus, measured densities are within the expected range.

In addition, visual inspection was completed to reveal some possible structural cracks, apart from drying shrinkage, which can affect the test results. During the testing process, the load was applied at a constant rate and the maximum load was reached within considerable time. To calculate the compressive strength for each specimen, the following equation was used:

$$UCS = \frac{P}{A}$$

where:

UCS – Unconfined Compressive Strength, MPa

P – maximum load recorded, kN

A – the cross-section area of the specimen, mm^2

Figure 5-5 demonstrates test setup and frame of the UCS test in the CPATT lab.

(a)

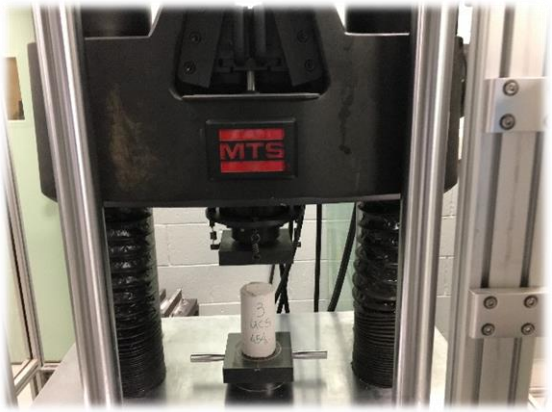

(b)

(c)

Figure 5-5: Unconfined Compressive Strength. (a) - samples, ready to be tested; (b) and (c) - testing equipment

The UCS test was performed at 7, 14, 21, and 28 days at the CPATT laboratory. Figures 5-6 and 5-7 show the results from UCS test varies as low as 1.27 MPa to as high as 1.69 MPa. For 7 days and 28 days, the compressive strength was relatively consistent and stayed in the ranges of 1.37 to 1.61 MPa and 1.51 to 1.55 MPa respectively. One of the issues with the testing process was an insufficient number of samples for the 28 days UCS test – only two of them were correctly tested and results were obtained. Following the ASTM C495 procedure, four samples have to be tested in order to obtain reliable results. In addition, a few samples were needed for each testing day in order to calibrate the test frame. Also, a few samples were damaged during the curing period, while on site. Samples were left on site at the ambient temperature during the first three days and were discovered lying on the ground when it was time to pick the samples up from the site. Visually, cracks were observed later on the surface of some samples, but it was hard to say if those cracks were drying shrinkage cracks or some structural cracks. Those damaged samples were not tested to avoid confusion. Some of them were used as "dummy" samples, but overall number was already insufficient to have four good quality samples for 28 days UCS testing. UCS test results for 7, 14, 21 and 28 days are presented in Figure 5-6. The data for the testing are presented in Appendix III.

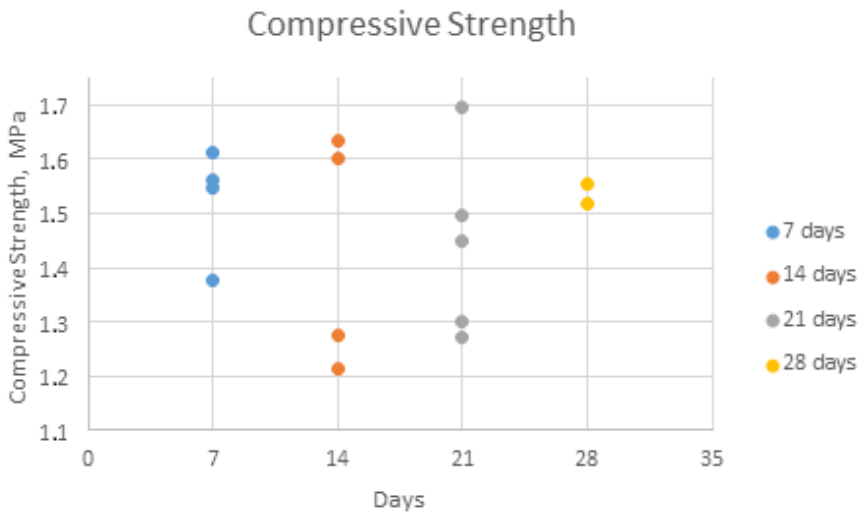

Figure 5-6: UCS Test Results

After calculating the average values for each sample age, 7, 14, 21 and 28 days, the compressive strength was determined to be within a small range throughout all the ages of the samples (Figure 5-7). The fluctuation of the results was from 1.44 MPa to 1.53 MPa, meaning no significant difference was observed between 7, 14, 21 and 28 days samples.

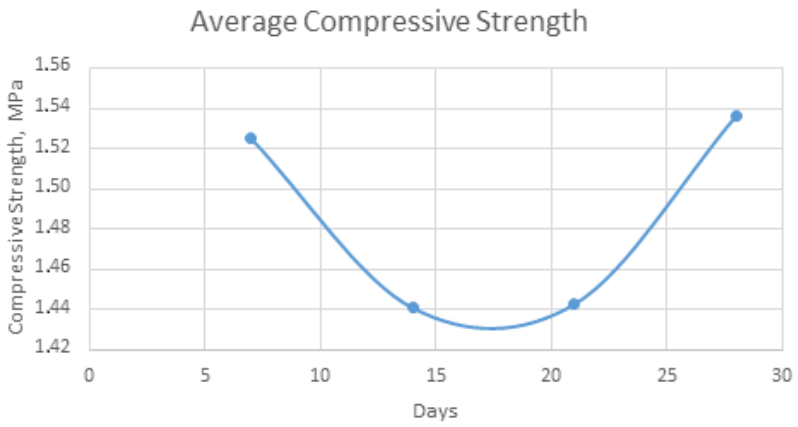

Figure 5-7: Average UCS Test Results

Table 5-1 presents typical values for Cellular Concrete. For the densities between 400 and 600 kg/m^3, compressive strength ranges from 0.5 to 1.5 MPa. Those are the approximate values and the range for compressive strength is relatively large because it may include the cellular concrete with different mix compositions. The target density of the samples, taken from the site in Toronto, was 475 kg/m^3. This means that the results were more than satisfied and material cast in-situ has gained relatively high compressive strength for its density.

Table 5-1: Typical Properties of Cellular Concrete Based on British Concrete Association (BCA 1994)

Dry Density (kg/m^3)	Compressive Strength (MPa)	Drying Shrinkage (%)	Modulus of Elasticity (MPa)	Thermal Conductivity (W/mK)
400	0.5-1.0	0.30-0.35	800-1,000	0.10
600	1.0-1.5	0.22-0.25	1,000-1,500	0.11
800	1.5-2.0	0.20-0.22	2,000-2,500	0.17-0.23
1000	2.5-3.0	0.15-0.18	2,500-3,000	0.23-0.30
1200	4.5-5.5	0.09-0.11	3,500-4,000	0.38-0.42
1400	6.0-8.0	0.07-0.09	5,000-6,000	0.50-0.55
1600	7.5-10.0	0.06-0.07	10,000-12,000	0.62-0.66

5.4.2 **Modulus of Elasticity and Poisson's Ratio**

The testing method was completed in accordance with ASTM C469. The dimension of the specimen was 150 mm by 300 mm for the samples with targeted 475 kg/m^3 density. Before testing the samples, they were grinded at the top and the bottom in order to have horizontal flat surfaces. Measurements of the samples were taken such as height, diameter, and weight. In addition, visual inspection was completed to reveal some possible structural cracks, apart from drying shrinkage, which can affect the test results. The same as for the compressive strength, actual density of the samples was calculated by dividing the weight of the sample to its volume. The average hardened state density appeared to be slightly higher than one in the smaller samples (for UCS test) and it was reported as 417 kg/m^3 for this batch of samples.

The configuration of the test apparatus is shown in Figure 5-8. The calculation of the two parameters are described as follows:

- For Modulus of Elasticity:

$$E = \frac{(S_2 - S_1)}{(\varepsilon_2 - 0.000050)}$$

where:

E – modulus of elasticity, MPa

S_2 – stress corresponding to 40% of ultimate load, MPa

S_1 – stress corresponding to a longitudinal strain, ε_2 , of 50 million, MPa

ε_2 – longitudinal strain produced by stress S_2

- For Poisson's ratio:

$$\mu = \frac{(\varepsilon_{t2} - \varepsilon_{t1})}{(\varepsilon_2 - 0.000050)}$$

where:

μ - Poisson's ratio

ε_{t2} – transverse strain at midheight of the specimen produced by stress S_2

ε_{t1} – transverse strain at midheight of the specimen produced by stress S_1

Figure 5-8: Modulus of Elasticity and Poisson's Ratio Test Setup

Prior to the actual test, two specimens were tested to determine the compressive strength. The 40% of the maximum load was determined in this trial test, which then was used as the maximum load for the modulus of elasticity test. The compressometer and extensometer were used to measure the modulus of elasticity and Poisson's ratio as they provide readings for longitudinal strain and transverse strain. In accordance to ASTM C469, the sample should be loaded no less than three times and the first reading is not recorded as valid. During the test at the CPATT lab, each of the three samples was loaded six times, but the first reading was not taken into account since it is considered as a trial loading (according to the ASTM C469). Results are presented in Figure 5-9. Samples were tested at 28 days.

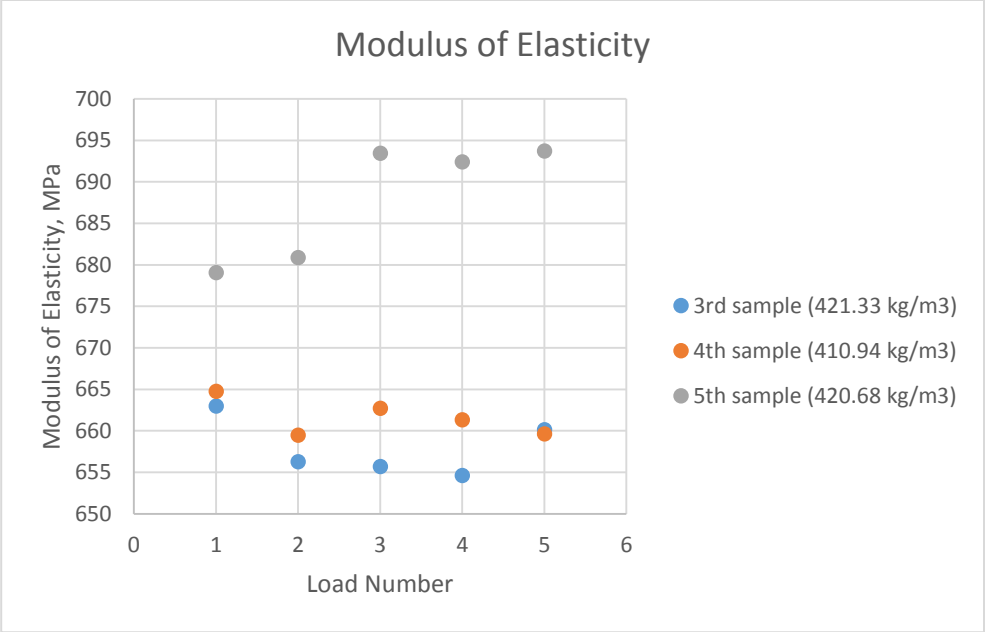

Figure 5-9: Modulus of Elasticity Test Results for 28 Days Samples

The average modulus of elasticity was determined as 657, 661 and 687 MPa for the 3rd, 4th, and 5th samples respectively. The result for modulus of elasticity for the 5th sample was obtained to be the highest, corresponding to the 420.68 kg/m^3 density, whereas for the 3rd sample modulus of elasticity was determined as the lowest with the sample density at 421.33 kg/m^3 (Figure 5-9). During the testing of the 5th sample, it was found that the reading increased from 680 to 693 MPa after the second cycle. This may be explained due to the fact that the test frame had some noise during testing and several adjustments were made to the longitudinal extensometer. According to Table 5-1, the lower limit for modulus of elasticity of the 400 kg/m^3 density is approximately 800 MPa, whereas laboratory results observed it to be in the range of 657 to 687 MPa.

The Poisson's ratio was observed in the range of 0.24 to 0.30 (Appendix III), which is consistent to the past literature (BCA, 1994).

5.4.3 Relationship between Properties

Correlation between compressive strength and density is shown in Figure 5-10. The trend for 7 days samples was not typical because the lower density was observed, the higher compressive strength was, though 7 days samples had a good R^2 value of 0.96. For the 14 and 21 days samples with hardened state density of 404 to 414 kg/m^3 the range of the compressive strength was relatively different, laying in the range of 1.2 to 1.69 MPa. For the 28 days samples, despite the expectations, compressive strength was observed to be at approximately same level as for other days samples (1.52 to 1.55MPa).

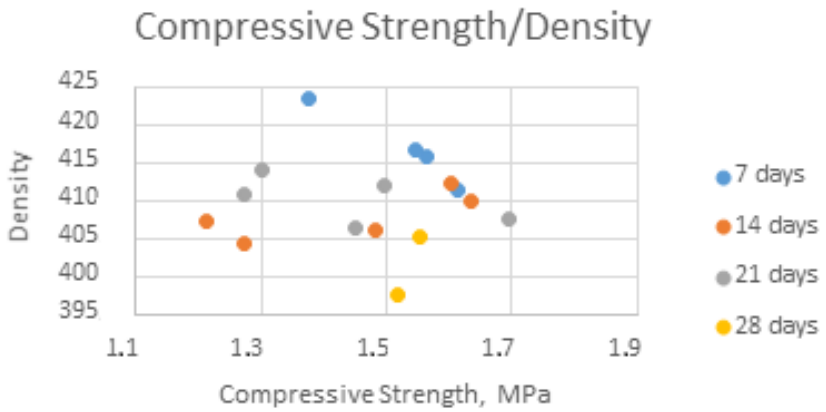

Figure 5-10: Correlation of Compressive Strength and Density

5.5 Summary

It is worth mentioning that one of the hypothesis of the thesis was that the mechanical properties of the site cast samples would be different from the typical values. As a result of the laboratory testing, some mechanical properties were different from the ones in the literature.

- The field cast samples usually have completely different curing procedure. Because of the high temperatures during the curing period, it is assumed that samples gained high strength in the first few days.
- Obtained results may be the reason of possibly damaged bubbled structure as none of the vibration should be done to the material although in order to test the samples they were transported to the laboratory on the 4th day. There is no specific requirement on after what day samples can be transported.
- For field cast samples correlation between compressive strength and modulus of elasticity was not found as strong. This could be studied more thoroughly by collecting more samples, thus having a greater data set.
- High compressive strength values, especially on early stages (before 28 days) may be the result of using good quality material in the field by CEMATRIX.

CHAPTER 6

6 CONCLUSIONS AND FUTURE RECOMMENDATIONS

6.1 Conclusions

Lightweight Cellular Concrete (LCC) is a lightweight product, consisting of Portland Cement, water, and foaming agent which contain air bubbles. LCC is relatively homogeneous compared to conventional concrete, as it does not contain coarse aggregate. It has constructive advantages such as low density with higher pound for pound strength compared with natural concrete and other fill materials. The properties of LCC depend on its microstructure and composition, methods of pore-formation and curing. Apart from being lightweight, LCC is a cost-effective and sustainable material and has superior thermal properties, freeze-thaw resistance, and good flowability. It can be used in a number of applications including but not limited to backfill, soil stabilization, embankment fills and pipe bedding, but this research was focused on studying of this material as an alternative construction material for reducing the weight of the subbase in pavement engineering, thereby mitigating excessive settlements and bearing failures.

In terms of insulation value, LCC also has energy absorbing, thermal insulating, and soundproofing properties. The air voids are homogeneously distributed within LCC and by utilizing the LCC within the roadway structure, pavement damage from frost heave and spring thaw softening are reduced.

This material is potentially cost-effective both in the short and long term. LCC typically replaces granular subbases two-to-three-times greater in thickness; therefore, less underlying soil needs to be excavated.

LCC also has environmental benefits, as it is inert and non-contaminating compared to other potential lightweight materials, and uses relatively easily available materials. It can also include industrial byproducts and waste materials such as fly ash. It is relatively inexpensive, easy to make, and easy to use. It is versatile in that it can be pumped into place and poured into complex forms.

With a greater emphasis on sustainability, materials such as LCC can minimize the generation of waste and deliver better performing pavements that require less maintenance.

The major conclusions drawn from this research are outlined in the following section:

- According to the report and visual inspection that were done at the Dixie Road, no significant transverse and longitudinal cracks were observed. Both, Winston Churchill Boulevard and Highway 9 sections are in good condition with no visual distresses. The

bus-lane in Calgary (the oldest section) is performing well. No recent data from the road section in British Columbia was collected.

- The inspections were done after the construction on the studied sections at different times. The results of the visual inspection, Falling Weight Deflectometer (FWD) as well as Benkelman Beam Test (for some cases) showed that the road sections are performing well and have some minor distresses on the surface (Dixie Road). FWD and Benkelman Beam Test are the most common tests for evaluating performance.
- However, in-depth pavement data collection must be complete to provide a comprehensive review of the performance of the sections with LCC as a subbase layer. Therefore, further investigation is recommended. This could be achieved by using pavement instrumentation such as asphalt gauges, earth pressure cells, and environmental equipment.
- In order to use LCC in a pavement structure as a subbase, certain activities have to be taken into consideration and implemented into the construction process. A number of general observations that are applicable to most LCC projects have been made from studying the road sections across Canada. These recommended construction activities include controlling the water table, constructing the proper drainage, transition areas between the sections and using quality equipment and professional personnel.
- It is clear from the failure criteria analysis that the pavement with LCC subbase is more durable than the pavement with Granular B layer at the same thicknesses.
- The result of the failure criteria analysis indicated that the pavement thickness using LCC as a subbase material could be thinner than the conventional pavement, which reduces the excavation depth during the construction and saves time and cost.
- The WESLEA software does not consider the environmental impact of temperature and moisture. In-situ field inspection is needed to evaluate the environmental effect on the pavement using LCC as a subbase layer.
- The mechanical properties of the site cast samples were found to be different from the typical values in the literature.
- For field cast samples correlation between the compressive strength and modulus of elasticity were not highly correlated. This could be studied more thoroughly by collecting more samples to obtain more data.
- The use of LCC as a pavement subbase layer could be practical and feasible in particular scenarios.

6.2 Future Recommendations

In terms of disadvantages of LCC, its high flowability means LCC must typically be placed into forms and cannot have a surface slope of more than 1 degree. Due to its low density, upward buoyancy forces must be taken into account if the concrete is expected to be submerged

in water. Its initial cost may be higher, depending on the density and composition. This area may also need clarification and analysis in the future

Based on this research, the following are recommended areas for future work:

- New road sections must be built to provide data collection opportunities for researchers regarding LCC performance.
- Those new pavements may be equipped with instrumentation such as earth pressure cell, horizontal strain gauge, and vertical strain gauge. This will help to quantitatively estimate pavement performance and will serve as a solid base for its evaluation.
- More in-depth study of the LCC properties is required.
- Correlation between laboratory and field cast samples could be determined in order to understand the effect of curing conditions and the quality of the material in general.
- LCC has many potential benefits in terms of sustainability in construction such as low ease of application, reduction in use of virgin materials, using by-products as a substitute to cement, for example. In order to evaluate and calculate those benefits, Life Cycle Cost Assessment and Life Cycle Cost Analysis must be performed, which was not accomplished in the past studies.

REFERENCES

Aldridge, D. (2005). Introduction to foamed concrete: what, why, how? In Use of Foamed Concrete in Construction: Proceedings of the International Conference held at the University of Dundee, Scotland, UK on 5 July 2005 (pp. 1-14). *Thomas Telford Publishing.*

American Society for Testing and Materials (ASTM) C796/C796M. (2012). Standard Test Method for Foaming Agents for Use in Producing Cellular Concrete Using Preformed Foam.

American Society for Testing and Materials (ASTM) D4694-09 (2015). Standard Test Method for Deflections with a Falling-Weight-Type Impulse Load Device.

American Society for Testing and Materials (ASTM) D4695-03 (2015). *Standard Guide for General Pavement Deflection Measurements.*

American Society for Testing and Materials (ASTM) D6433 – 18 (2012). Standard Practice for Roads and Parking Lots Pavement Condition Index Surveys.

Amran, Y. M., Farzadnia, N., and Ali, A. A. (2015). Properties and applications of foamed concrete; a review. *Construction and Building Materials*, 101, 990-1005.

Applied Research Associates ARA (2015) Methodology for the Development of Equivalent Pavement Structural Design Matrix for Municipal Roadways.

Arulrajah, A., Disfani, M. M., Maghoolpilehrood, F., Horpibulsuk, S., Udonchai, A., Imteaz, M., and Du, Y. J. (2015). Engineering and environmental properties of foamed recycled glass as a lightweight engineering material. *Journal of Cleaner Production*, 94, 369-375.

Awang, H., Aljoumaily, Z. S., Noordin, N., & Al-Mulali, M. Z. (2014). The Mechanical Properties of Foamed Concrete containing Un-processed Blast Furnace Slag. *In MATEC Web of Conferences (Vol. 15, p. 01034). EDP Sciences*.

British Cement Association (BCA) (1994). "*Foamed concrete - Composition and properties". First published in 1991*, British Cement Association.

Brady, K. C., Jones, M. R., & Watts, G. R. (2001). Specification for foamed concrete. TRL Limited.

Byun, K. J., Song, H. W., Park, S. S., & Song, Y. C. (1998). Development of structural lightweight foamed concrete using polymer foam agent. ICPIC-98, 9.

Darshan, M. (2016). Comparison on Auto Aerated Concrete to Normal Concrete. *GRD Journals, Global Research and Development Journal for Engineering, 5*.

Dolton, B., Witchard, M., Luzzi, D., & Smith, T. J. (2016). Application of Lightweight Cellular Concrete to Reconstruction of Settlement Prone Roadways in Victoria. *GEOVancouver*.

Dransfield, J. M. (2000, March). Foamed concrete: Introduction to the product and its properties. In One-day awareness seminar on Foamed Concrete: Properties, Applications and Potential, University of Dundee, Scotland (pp. 1-11).

Friesen, J., Adedapo, D., Kenyon, R., & Eden, R. J. (2012). Bridge Embankment Stabilization in Deep Soft Lacustrine Clays Under High Artesian Pressures. *GEOManitoba*.

Golder Associates (2008). Technical Memorandum. View Street and Vancouver Street, Victoria. Benkelman Beam Testing and Falling Weight Deflectometer Testing.

Griffiths F. and Popik, M. (2013). Pavement Evaluation - CEMATRIX Site Dixie Road, Caledon, Ontario. Thurber Engineering Ltd. 2010 Winston Park Drive, Oakville, ON.

Hoff Inge, Watn A, Oiseth E, EMDAL A., Amundsgard, K O., (2002). Light Weight Aggregate (LWA) Used In Road Pavements. Proceedings of the 6th international conference on the bearing capacity of roads and airfields, Lisbon, Portugal, 2, pp. 1013-22.

Horpibulsuk, S., Suddeepong, A., Suksiripattanapong, C., Chinkulkijniwat, A., Arulrajah, A., & Disfani, M. M. (2014). Water-void to cement ratio identity of lightweight cellular-cemented material. Journal of Materials in Civil Engineering, 26(10), 06014021.

Jones M.R., (2001). Foamed concrete for structural use. Proceedings of one-day seminar on foamed concrete: properties, applications, and latest technological developments. Loughborough University, pp. 27–60.

Jones, M.R., & McCarthy, A. (2005). Utilising unprocessed low-lime coal fly ash in foamed concrete. Fuel, 84(11), 1398-1409.

Jones, M.R., & McCarthy, A. (2005). Preliminary views on the potential of foamed concrete as a structural material. *Magazine of concrete research*, 57(1), 21-31.

Jones, M.R., & McCarthy, A. (2006). Heat of hydration in foamed concrete: Effect of mix constituents and plastic density. *Cement and concrete research*, 36(6), 1032-1041.

Jones, M.R., Zheng, L., Yerramala, A., Rao, K.S. (2012). Use of recycled and secondary aggregates in foamed concrete. *Magazine of Concrete Research*, 64(6), pp. 513-525.

Jones, M.R., Ozlutas, K., & Zheng, L. (2016). Stability and instability of foamed concrete. *Magazine of Concrete Research*, 68(11), 542-549.

Jones, M. R., Ozlutas, K., & Zheng, L. (2017). High-volume, ultra-low-density fly ash foamed concrete. *Magazine of Concrete Research*, 1-11.

Kadela, M., Kozłowski, M., & Kukiełka, A. (2017). Application of foamed concrete in road pavement–weak soil system. *Procedia Engineering*, 193, 439-446.

Kearsley, E.P. (1996) The Use of Foamed Concrete for Affordable Development in Third World Countries. *In Appropriate Concrete Technology; Dhir, R.K., McCarthy, M.J., Eds.; E & FN Spon: London, UK*, pp. 233–243

Kearsley E.P., Wainwright P.J. (2001). The effect of high fly ash content on the compressive strength of foamed concrete. *Cement Concrete Research*, 31, pp. 105–12.

Kearsley E.P, Wainwright PJ (2002). Ash content for optimum strength of foamed concrete. *Cement Concrete Research*, 32, pp. 241–6

Khayat, K. H., & Assaad, J. (2002). Air-void stability in self-consolidating concrete. *ACI Materials Journal*, 99(4), 408-416.

Koudriashoff IT (1949). Manufacture of reinforced foam concrete roof slabs. *J Am Concr Inst*, 21(1), pp. 37–48.

Lee, Y. L., Goh, K. S., Koh, H. B., & Bakar, I. (2009). Foamed aggregate pervious concrete–an option for road on peat.

Legatski, L. A. (1994). Cellular concrete. In *Significance of Tests and Properties of Concrete and Concrete-Making Materials*. ASTM International.Loewen, E. B., Baril, M., & Eric, R. (2012). Rapid Design and Construction of an Integral Abutment Bridge with MSE Walls and Cellular Concrete Backfill. *Conference of the Transportation Association of Canada.*

Maher, M. L., & Hagan, J. B. (2016). Constructability Benefits of Using Lightweight Foamed Concrete Fill in Pavement Applications. *CSCE Annual Conference, London*.

McGovern, G. (2000, March). Manufacture and supply of ready-mix foamed concrete. In One Day Awareness Seminar on Foamed Concrete: Properties, Applications and Potential, University of Dundee, Scotland (pp. 12-25).

Mohammad, M. (2011). Development of foamed concrete: enabling and supporting design *(Doctoral dissertation, School of Engineering, Physics and Mathematics).*

Nambiar, E.K.K., Ramamurthy, K. (2006). 'Influence of filler type on the properties of foam concrete'. *Cement and concrete composites, Vol.28*, pp. 475-480.

Narayanan, N., & Ramamurthy, K. (2000). Structure and properties of aerated concrete: a review. *Cement and Concrete Composites*, 22(5), 321-329.

Neville, A. M. (2011). Properties of concrete. *5th edition, Pearson Education Ltd*.

Oginni, F. A. (2015). Continental application of foamed concrete technology: Lessons for infrastructural development in Africa. British *Journal of Applied Science & Technology*, 5(4), 417.

Ozlutas, K. (2015). Behavior of ultra-low density foamed concrete *(Doctoral dissertation, University of Dundee).*

Ramamurthy, K., Nambiar, E. K., & Ranjani, G. I. S. (2009). A classification of studies on properties of foam concrete. *Cement and Concrete Composites*, 31(6), 388-396.

Raphael, J. M. (1984, March). Tensile strength of concrete. In Journal Proceedings (Vol. 81, No. 2, pp. 158-165).

Sabir, B. B., Wild, S., & O'farrell, M. (1998). A water sorptivity test for mortar and concrete. *Materials and Structures*, 31(8), 568.

Sari, K. A. M., & Sani, A. R. M. (2017). Applications of Foamed Lightweight Concrete. *In MATEC Web of Conferences* (Vol. 97, p. 01097). *EDP Sciences*.

Taylor, R., Eric, R., Wiebe, D., & Loewen, S. (2016). Waverly West Arterial Roads Project Kenaston Overpass. *Conference of the Transportation Association of Canada.*

Tiwari, B. *et al.* (2017) 'Mechanical Properties of Lightweight Cellular Concrete for Geotechnical Applications', *Journal of Materials in Civil Engineering*, 29(7), p. 6017007. doi: 10.1061/(ASCE)MT.1943-5533.0001885.

Transportation Association of Canada –TAC (2013). Transport Asset Design and Management Guide.

Transportation Association of Canada TAC (2014) Default Parameters for AASHTOWare Pavement ME Design Canadian Guide.

Valore, R. C. (1954b). Cellular concretes part 2 physical properties. *In Journal Proceedings* (Vol. 50, No. 6, pp. 817-836).

Valore, R. C. (1954a). Cellular concretes Part 1 composition and methods of preparation. *In Journal Proceedings* (Vol. 50, No. 5, pp. 773-796).

Van Deijk, S. (1919). Foam concrete. *Concrete*, 25(5).

Wei, S., Yigiang, C., Yunsheng, Z., Jones, M.R. (2013). "Characterization and simulation of microstructure and thermal properties of foamed concrete*". Construction and Building Materials,* 47, pp. 1278-1291.

WCED, (1987).Our Common Future. *World Commission on Environment and Development*. Oxford University Press, Oxford.

Yakovlev, G., Kerienė, J., Gailius, A., & Girnienė, I. (2006). Cement based foam concrete reinforced by carbon nanotubes. *Materials Science [Medžiagotyra], 12*(2), 147-151.

APPENDIX I

FWD Dixie Road Data

Station (km)	Layer Thickness (mm)			ND (microns	E_s (MPa)	M_R (MPa)	E_P (MPa)	SN_{Eff} (mm)	LCC Structural Coefficient
	Asphalt	Base	Subbase						
Dixie Road Northbound Lane									
10+280	137	150	400	201	200	66	860	154	
10+285	137	150	400	229	179	59	749	148	
10+290	137	150	400	248	197	65	650	141	
10+292	137	150	400	269	186	61	596	137	
10+294	137	150	400	303	203	67	495	129	
10+296	137	148	650	239	194	64	639	190	0.185
10+298	135	129	650	260	197	65	575	180	0.173
10+300	133	122	650	248	220	73	595	180	0.176
10+310	157	119	650	231	139	46	736	198	0.19
10+320	142	128	650	444	69	23	389	159	0.138
10+330	145	95	650	446	53	17	434	159	0.143
10+340	151	106	650	316	68	22	636	184	0.176
10+350	149	97	650	273	77	25	747	192	0.19
10+360	151	71	650	271	96	32	700	183	0.18
10+370	146	109	650	197	102	34	1055	218	0.229
10+380	159	97	650	205	96	32	1017	215	0.22
10+390	135	122	650	267	76	25	770	196	0.201
10+400	130	115	650	274	159	52	570	175	0.173
10+410	152	91	650	189	218	72	844	199	0.201
10+415	155	97	650	206	234	77	741	193	0.188
10+417	155	152	650	164	237	78	970	224	0.226
10+419	155	184	650	188	241	80	810	218	0.211
10+421	155	184	650	197	224	74	775	215	0.206
10+423	155	202	650	263	197	65	557	196	0.173
10+425	155	150	400	287	178	59	552	137	
10+430	155	150	400	277	227	75	536	135	
10+435	155	150	400	306	267	88	454	128	
NB Approach			Average	250	193	64	670	142	
			Std Dev.	39	10	3	140	10	
NB Cematrix Site			Average	257	152	50	714	193	
			Std Dev.	77	69	23	180	19	
NB Leave			Average	290	224	74	514	133	
			Std Dev.	15	45	15	52	5	

Station (km)	Layer Thickness (mm)			ND (microns	E_s (MPa)	M_R (MPa)	E_P (MPa)	SN_{Eff} (mm)	LCC Structural Coefficient
	Asphalt	Base	Subbase						
Dixie Road - Southbound Lane									
10+280	150	150	400	271	225	74	554	136	
10+285	150	150	400	290	205	68	521	133	
10+290	150	150	400	284	261	86	501	132	
10+292	150	150	400	313	249	82	451	127	
10+294	152	150	400	307	220	73	476	130	
10+296	157	111	650	229	225	74	649	188	0.177
10+298	157	117	650	201	219	72	771	200	0.195
10+300	155	111	650	194	225	74	805	201	0.199
10+310	149	111	650	205	199	66	774	198	0.196
10+320	141	132	650	276	108	36	632	187	0.181
10+330	138	128	650	385	56	19	514	174	0.163
10+340	144	131	650	226	88	29	907	212	0.217
10+350	143	103	650	248	115	38	725	190	0.19
10+360	149	99	650	208	128	42	887	204	0.208
10+370	150	89	650	198	115	38	994	210	0.218
10+380	140	100	650	206	115	38	942	206	0.217
10+390	130	143	650	227	112	37	818	204	0.211
10+400	164	109	650	235	99	33	817	204	0.198
10+410	132	197	650	208	171	56	779	213	0.214
10+415	131	195	650	236	185	61	650	200	0.195
10+417	138	203	650	214	214	71	705	208	0.203
10+419	148	220	650	220	192	63	696	213	0.201
10+421	160	212	650	195	202	67	796	224	0.212
10+423	168	224	650	238	188	62	633	212	0.186
10+425	175	150	400	253	183	60	639	148	
10+430	160	150	400	253	189	62	636	144	
10+435	150	150	400	316	179	59	485	130	
SB Approach			Average	251	188	62	638	171	
			Std Dev.	43	9	3	110	43	
SB Cematrix Site			Average	239	160	53	737	193	
			Std Dev.	49	58	19	151	25	
SB Leave			Average	282	230	76	526	134	
			Std Dev.	10	28	9	27	2	

APPENDIX II

TYPICAL PAVEMENT SURFACE TEMPERATURE IN SOUTHERN AND EASTERN ONTARIO

Month	1st Quintile (°C)	2nd Quintile (°C)	3rd Quintile (°C)	4th Quintile (°C)	5th Quintile (°C)	Mean Temp. (°C)	Std. Dev. (°C)
January	-13.0	-8.4	-5.5	-2.9	0.3	-5.9	4.8
February	-13.2	-8.7	-5.5	-2.7	1.4	-5.7	5.2
March	-7.9	-3.4	-0.6	2.3	7.3	-0.4	5.4
April	-1.1	3.3	6.7	10.7	17.4	7.4	6.7
May	5.2	10.4	14.1	18.4	26.0	14.8	7.4
June	11.9	16.9	20.7	25.2	32.4	21.4	7.3
July	14.6	19.6	23.4	27.8	34.4	23.9	7.1
August	13.3	17.9	21.3	25.6	32.1	22.1	6.7
September	8.3	13.1	16.6	20.3	26.7	17.0	6.6
October	2.8	6.8	9.9	13.3	19.2	10.4	5.9
November	-2.2	1.1	3.1	5.3	9.1	3.2	4.1
December	-9.3	-5.4	-3.1	-0.7	2.8	-3.1	4.3

APPENDIX III

DATA FOR

LABORATORY TESTING

7 days

Date cast	Date Tested	Code	Casted Density (kg/m^3)	Average Diameter (mm)	Average Height (mm)	volume (mm^3)	Weight of Specimen (g)	Applied Load (KN)	Surface Area (mm2)	Comp. Strength (MPa)	Actual density (kg/m3)
25-May-18	1-Jun-18	3	475	75,910	146,590	663425,574	276	7,072427	4525,722	1,563	416,023
		4		76,250	146,300	668057,592	283	6,286667	4566,354	1,377	423,616
		5		76,305	142,420	651278,672	268	7,375137	4572,944	1,613	411,498
		6		76,190	143,680	655061,609	273	7,052352	4559,170	1,547	416,755

14 days

25-May-18	8-Jun-18	1	475	76,325	144,595	661571,492	272,8	7,326274	4575,341	1,601	412,352
		2		76,435	150,085	688670,866	282,3	7,492442	4588,539	1,633	409,920
		3		76,520	146,995	675993,261	275,4	5,576168	4598,750	1,213	407,401
		4		76,320	145,860	667271,866	269,8	5,829073	4574,742	1,274	404,333
		5		76,425	144,245	661700,624	269,2		4587,338	0,000	406,831
		6		76,465	147,985	679568,068	276	6,810149	4592,142	1,483	406,140

21 days

25-May-18	15-Jun-18	1	475	77,14	76,840	151,020	151,280	701529,777	285,2	6,721827	4637,294	1,450	406,540
				76,54		151,540							
		2		77,05	76,645	150,490	150,575	694720,973	285,4	5,870159	4613,787	1,272	410,812
				76,24		150,660							
		3		76,96	76,615	149,610	149,615	689751,463	285,6	5,994846	4610,176	1,300	414,062
				76,27		149,620							
		4		77,44	76,825	147,850	147,605	684220,510	285,3	6,750173	4635,483	1,456	416,971
				76,21		147,360							
		5		76,25	76,170	151,290	151,280	689349,252	281	7,730247	4556,777	1,696	407,631
				76,09		151,270							
		6		76,72	76,220	151,340	151,000	688976,989	283,9	6,824816	4562,762	1,496	412,060
				75,720		150,660							

28 days

25-May-18	22-Jun-18	1	475	76,12	76,140	146,950	146,920	668954,448	271,2	7,073447	4553,188	1,554	405,409
				76,16		146,890							
		2		76,16	76,220	149,760	149,820	683592,931	271,9	6,932021	4562,762	1,519	397,751
				76,28		149,880							

	Height	average	Diameter	average	Weight	ultimate load	Cycle	E	P	S1	S2	ε 2	ε t2	ε t1		E	average of 3 samples	P	average of 3 samples			Density
3	300,36	300,24	150,97	151,51	2,280,7	9,00	1	642,519396	-0,2729921	0,049773	0,477093	0,00071507	-0,000179	2,614E-06		657,9486		-0,28118		0,005413	2,281	421,33
	300,12		152,05				2	662,972431	-0,2711261	0,055746	0,47716	0,00068564	-0,000181	-8,325E-06								421,33
							3	656,295094	-0,2962172	0,057138	0,478145	0,00069149	-0,000193	-3,44E-06								421,33
							4	655,710551	-0,275486	0,056313	0,478632	0,00069406	-0,000191	-1,342E-05								421,33
							5	654,634951	-0,2767729	0,055863	0,478132	0,00069505	-0,000169	9,632E-06								421,33
							6	660,130068	-0,2862974	0,052951	0,479353	0,00069594	-0,0002	-1,493E-05								421,33
4	301,08	301,43	153,28	153,37	2,288,4	9,00	1	615,43521	-0,241753	0,054	0,462443	0,00071367	-0,000159	0,000001		661,5838		-0,24469		0,005569	2,288	410,94
	301,78		153,46				2	664,758994	-0,2373706	0,072788	0,466588	0,00064239	-0,000142	-1,359E-06								410,9365
							3	659,488162	-0,2365564	0,061116	0,465074	0,00066253	-0,000151	-6,049E-06								410,9365
							4	662,701418	-0,2536113	0,066985	0,455737	0,00063662	-0,000139	9,379E-06								410,9365
							5	661,320369	-0,2409747	0,063958	0,455644	0,00064228	-0,000141	1,903E-06								410,9365
							6	659,650138	-0,2578742	0,066265	0,45761	0,00064326	-0,000156	-2,719E-06								410,9365
5	301,02	300,73	151,88	151,94	2,293,8	9,00	1	667,210312	-0,3033913	0,043022	0,459577	0,00067432	-0,000191	-1,989E-06		687,9059		-0,28306		0,005453	2,294	420,68
	300,43		152,00				2	679,073003	-0,2991068	0,064895	0,475148	0,00065414	-0,000185	-4,322E-06								420,68
							3	680,879413	-0,2735181	0,057177	0,472678	0,00066024	-0,000177	-9,604E-06								420,68
							4	693,436836	-0,2587153	0,051636	0,476211	0,0006623	-0,0002	-3,77E-06								420,68
							5	692,415536	-0,2766003	0,050982	0,474138	0,00066113	-0,000165	4,116E-06								420,68
							6	693,724756	-0,2870394	0,058131	0,475953	0,00065229	-0,000177	-4,116E-06								420,68